Chapter 3:
Alteration, mineralisation, paragenesis and geological setting of epithermal deposits and prospects in the Seongsan district, South Korea

3.1 INTRODUCTION

This chapter documents the mineral assemblages, paragenetic relationships and geological settings of clay-sulfate and Au-Ag epithermal deposits and prospects in the Seongsan district.

Many of the alteration assemblages and paragenetic relationships are common to more than one prospect and so have been described together in the first part of this chapter rather than individually for each prospect. However, each prospect tends to have a different structural and stratigraphic setting and so the geological setting of each has been described separately in the latter part of the chapter.

The descriptions presented here allow each deposit and prospect to be compared with other epithermal systems. Based on the mineral assemblages, textures, paragenetic relationships and geological settings, correlations are made between the styles of epithermal systems in the Seongsan district and epithermal systems seen elsewhere.

Currently, it is unknown whether the clay-sulfate and nearby Au-Ag epithermal systems in the Seongsan district are related parts of a single metallogenic event, or one or more different events. The information presented in this chapter provides the geologic framework for subsequent geochronological (Chapter 4) and geochemical analyses (Chapter 5), which help to further understand the relationship between the clay-sulfate epithermal systems and nearby Au-Ag epithermal systems (Chapter 6).

Previous work in the Seongsan district has focussed on geochemical and geochronological studies of the clay-sulfate deposits at Seongsan and Ogmaesan (Chapter 1, Section 1.4), (Kim et al., 1990; Moon et al., 1990; Kim, 1991, 1992b, a; Kim et al., 1992; Kim & Nagao, 1992; Kim & Kusakabe 1993; Yoon, 1993, 1995; Koh, 1996; Koh & Chang, 1997; Koh et al., 2000; Choi et al., 2005). These workers identified extensive kaolinite-dickite and alunite alteration and have correlated the Seongsan and Ogmaesan deposits with high-sulfidation or acid-sulfate epithermal systems elsewhere. The advanced argillic zones in the Seongsan district are exploited as commercial sources of kaolinite and dickite rather than Au-Ag. Alunite has also been mined locally where sulfidation of the host rocks is particularly intense. Choi et al. (2005) provided brief descriptions of some aspects of the adularia-sericite Au-Ag epithermal systems at Eunsan and Moisan.

These previous workers paid little attention to the spatial or structural controls on hydrothermal activity or the likely location of any economically significant Au resource.

3.2 ALTERATION ASSEMBLAGES

Petrographic, x-ray diffraction (XRD) and microprobe analyses coupled with field mapping, and where available, diamond drill core logging were used to determine the extent of alteration assemblages. Staining of thin sections with sodium cobaltinitrite was also used to identify and map the distribution of potassium bearing feldspar. The form of individual crystals or overgrowths observed in thin section was used to distinguish adularia from orthoclase/microcline. Electron microprobe analyses were used to determine mineral compositions.

3.2.1 Primary mineral assemblages

Primary mineral assemblages in the Hwangsan Volcaniclastics unit (HV) in the Seongsan district include: quartz, plagioclase and biotite with lesser amounts of lithics; volcanic fragments of pumice, glass sphericules, fragments and shards; carbonaceous fragments; and, rare rutile, titanite and zircon. These primary minerals are preserved in samples peripheral to the various epithermal systems. However, it is rare to find any rock in the Seongsan district, either at surface or in drill core that has not undergone some alteration (Table 3-1).

3.2.2 Propylitic alteration

Propylitic alteration is recognised by the presence of albitised feldspar that is often partly replaced by carbonate in a matrix replaced by carbonate, inter-layered illite/smectite clays ± epidote ± chlorite (Fig. 3-1). Microprobe analyses of feldspars show that they have undergone complete albitisation with less than 3% anorthite remaining (electron microprobe data is presented after all of the alteration types have been discussed in Fig. 3-11).

3.2.3 Advanced argillic 1 alteration

Within each of the advanced argillic alteration assemblages (i.e. advanced argillic 1, 2 and 3), the matrix of the rock is generally comprised of variable amounts of very fine grained quartz, kaolinite, and/or dickite and/or alunite. Primary textures that may have been present within the original rock matrix have been largely obliterated. Scattered patches of coarser grained quartz, kaolinite, and/or dickite and/or alunite have shapes and sizes similar to outlines of euhedral feldspar and biotite phenocrysts still present in less altered rocks. The similarity of the shape and size of these coarser patches implies that they replaced phenocrysts whereas the finer material replaced the matrix. The texturally destructive nature of these advanced argillic alteration zones implies that advanced argillic alteration development was pervasive and shows that both matrix and rock components have been strongly altered.

Alteration types	Alteration assemblages
Propylitic	**albite, carbonate**, epidote, ±chlorite, ±illite/**smectite**
Advanced argillic 1	**kaolinite**, quartz, ±pyrite
Advanced argillic 2	**dickite**(kaolinite), quartz, ±pyrite
Advanced argillic 3	**alunite**, dickite(kaolinite), quartz
Siliceous[1]	**quartz** (by the addition of silica)
Silicic[2]	**quartz** (by loss of reactive components leaving residual silica)
Phyllic[3]	**illite/phengite (as muscovite-celadonite), pyrite**, ±quartz
Adularia	**adularia**, quartz, ±illite, ±pyrite
Carbonate (late-stage)	**carbonate**

Table 3-1 Alteration types and associated mineral assemblages observed in the Seongsan district. Alteration types (left column) are listed from generally the most to the least volumetrically abundant alteration type. Alteration mineral assemblages (right column) are listed from the most to the least commonly observed mineral within a given alteration type. Alteration minerals highlighted in bold signify key alteration mineral/s for each alteration type. **[1]** - the process of siliceous alteration is silicification. **[2]** - silicic alteration type is also commonly called residual silica, or vuggy silica. **[3]** – phyllic alteration type is also known as either 'sericite' or 'illite' alteration.

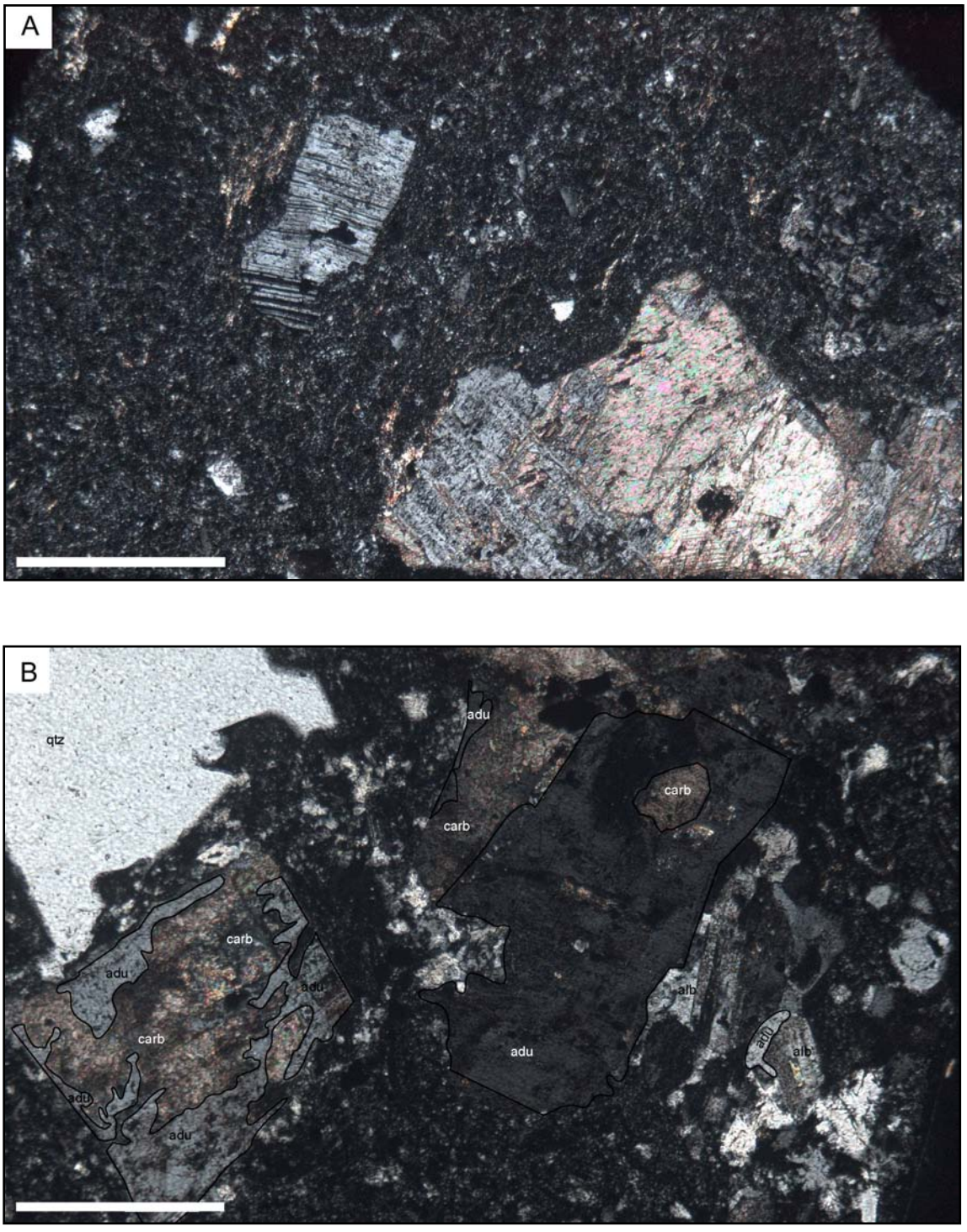

Fig. 3-1 Propylitic alteration in thin section. '**A**': example of propylitic altered sample showing completely albitised and carbonate-altered feldspar with overprinting very weakly developed phyllic alteration, evident as patchy illite replacement of the matrix (XPL, EN001 174m, scale bar 0.5mm). '**B**': relic propylitic alteration evident as albitised and carbonate-altered feldspar with phyllic and adularia-altered feldspar overprints (XPL, MS001 186.5m, scale bar = 0.25mm).

Advanced argillic 1 alteration comprises very fine-grained pervasive quartz+kaolinite and scattered patches of fine- to medium-grained quartz+kaolinite. Kaolinite generally forms very fine-grained plates inter-grown with each other and quartz (Fig. 3-2). Where zones of advanced argillic 1 alteration have sufficient purity and continuity, they are commonly exploited as commercial sources of kaolinite.

3.2.4 Advanced argillic 2 alteration

Advanced argillic 2 alteration comprises fine-grained pervasive quartz+dickite±pyrite and scattered patches of medium-grained quartz+dickite±pyrite. Dickite is distinguished from kaolinite in thin section as coarser plates (Fig. 3-2). Where zones of advanced argillic 2 alteration have sufficient purity of dickite/kaolinite and continuity, these zones are commonly exploited as commercial sources of dickite.

Disseminated massive sulfide and Au-Ag mineralisation are associated with advanced argillic 1 and 2 alteration locally (Fig. 3-3). Sulfide mineralisation is dominated by pyrite (Fig. 3-4). In addition, Ag-sulfides (argentite/acanthite), Ag-rich electrum inclusions in pyrite, Fe-poor sphalerite and galena also occur locally. Au-Ag and base metal mineralisation associated with advanced argillic 2 alteration is not developed beyond grades of 0.2ppm.

3.2.5 Advanced argillic 3 alteration

Advanced argillic 3 alteration comprises fine-grained pervasive quartz+alunite±kaolinite and scattered patches of medium-grained quartz+alunite±kaolinite. Alunite generally forms fine-grained laths inferred to represent part of the pervasive alteration of the rock matrix, or as medium- to coarse-grained laths that infill fractures and scattered patches that replace especially reactive components (Fig. 3-5). Where zones of advanced argillic 3 alteration have sufficient purity of alunite and continuity, they are commonly exploited as commercial sources of alunite.

Alunite from Seongsan and Ogmaesan were analysed to see if there was any compositional variation between or within the advanced argillic 3 alteration assemblage. Compositional variation in alunites is interpreted as an indication of specific environment or temperatures of formation (Deyell et at., 2005 and references within). End-member alunite is $KAl_3(SO_4)_2(OH)_6$ but can show substitution of K for Na, Ca, Ba, Sr, REE, Pb, substitution of Fe^{3+} for Al^{3+} and $(PO_4)^{3-}$ for $(SO_4)^{2-}$. The compositions of alunites from the Seongsan district were determined by examination of energy-dispersive spectra (EDS). Microprobe analyses were not able to be conducted due to a lack of standards for specific elements that were targeted. Multiple analyses (n=10) showed similar results, that the alunite compositions were uniform and that there was no significant substitution from end-member alunite (Fig. 3-6).

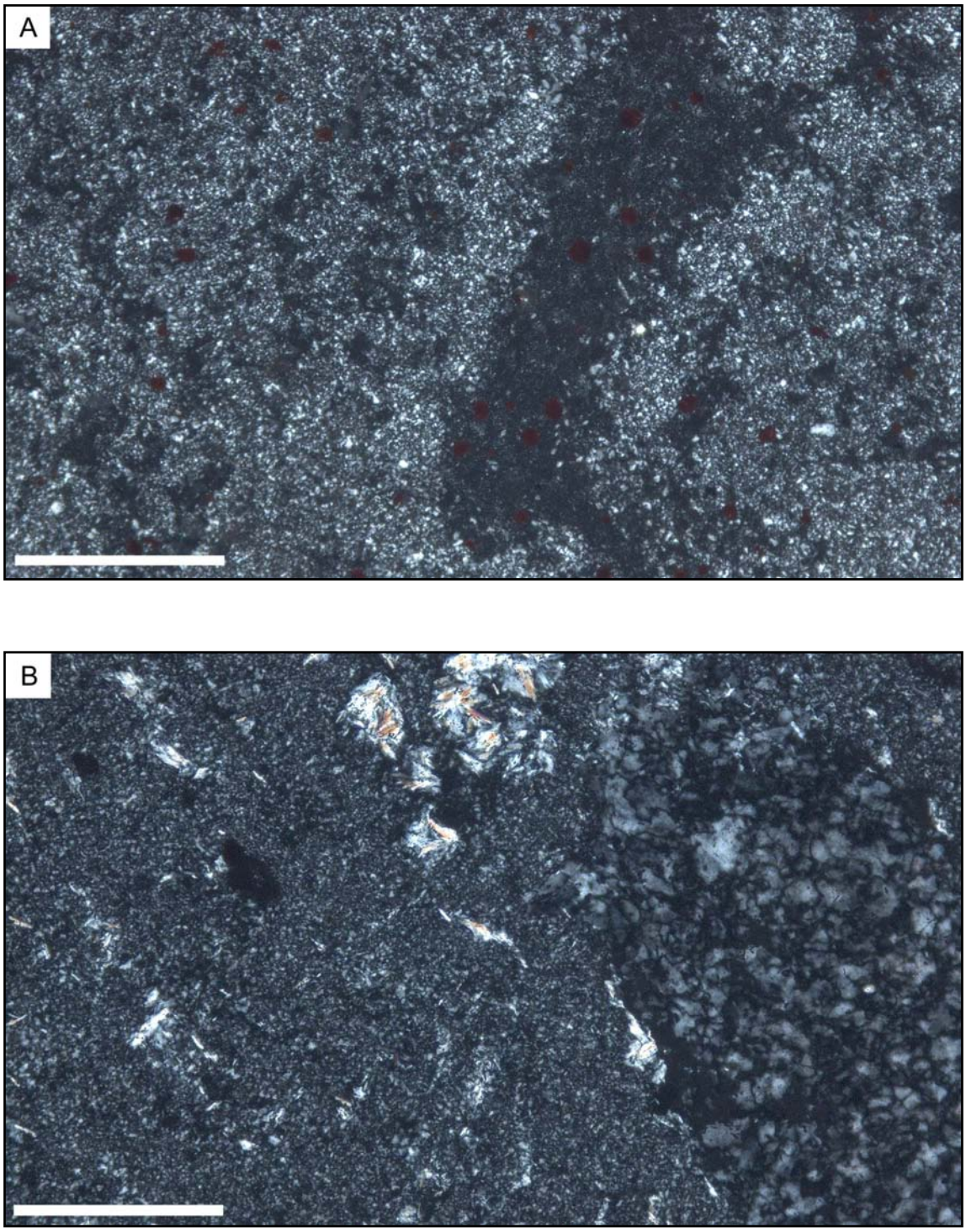

Fig. 3-2 Advanced argillic 1 and 2 alteration in thin section. '**A**': advanced argillic 1 alteration comprises predominantly quartz and kaolinite (dark mottled material) (XPL, sample location Ogmaesan ●*042*, scale bar = 0.25mm). '**B**': advanced argillic 2 alteration comprises quartz, kaolinite, minor alunite and dickite. The dark coarser material is dickite which is more crystalline and coarser than kaolinite in 'A' (XPL, sample location Ogmaesan ●*040*, scale bar = 0.25mm). 'A' and 'B' are both at the same scale, highlighting the increase in the clay minerals crystallinity and size between samples of advanced argillic 1 and advanced argillic 2 alteration.

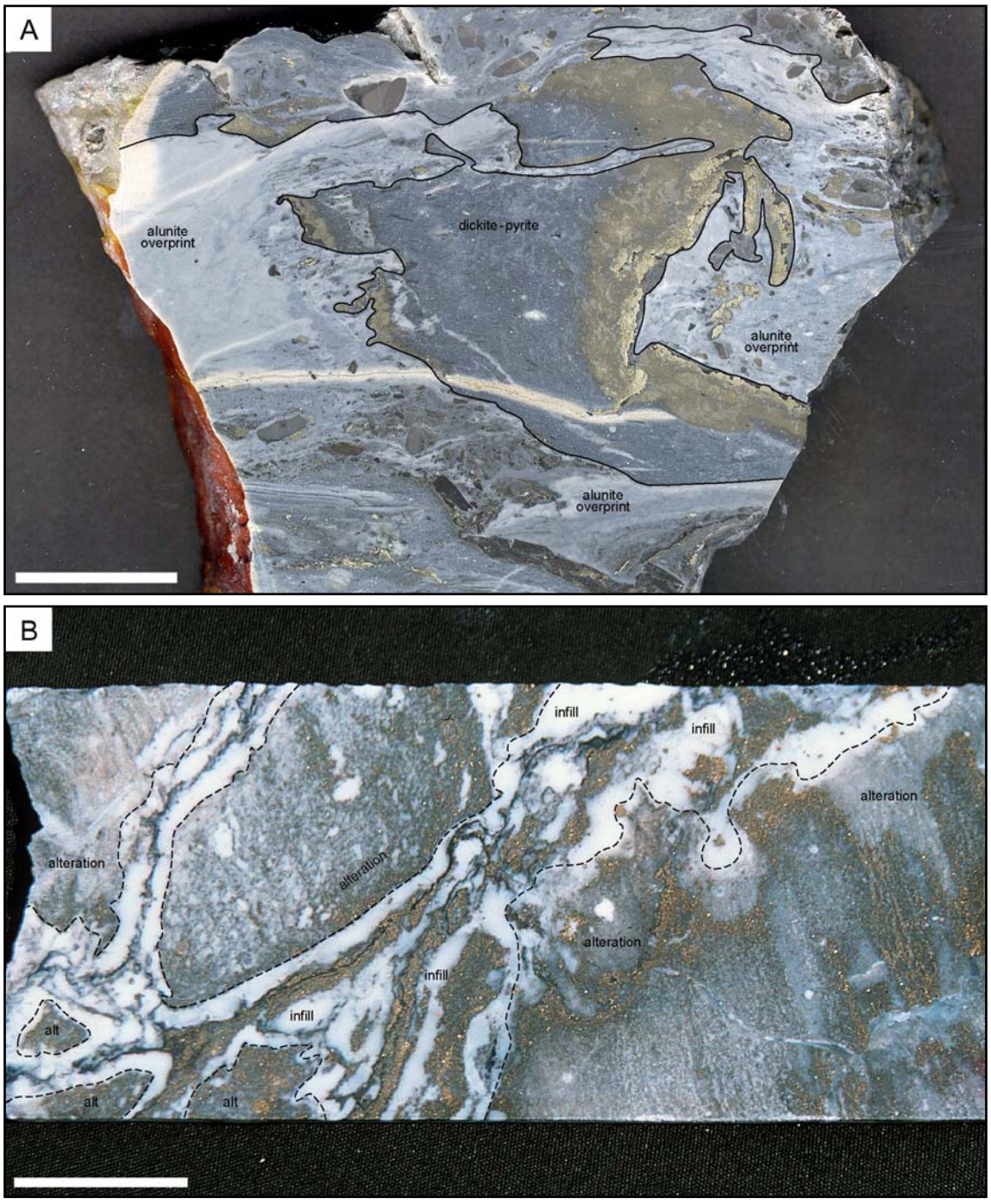

Fig. 3-3 Sulfide mineralisation associated with advanced argillic 2 alteration. '**A**': advanced argillic 2 dickite-pyrite alteration (central) forms darker grey zones richer in pyrite. The locally abundant zones of pyrite in this sample are selectively replacing reactive components within the host rock; the more diffuse pyrite is associated with dickite alteration. Both texturally distinct types of pyrite alteration are hosted within dickite alteration and field relationships consistently show that both are associated with dickite alteration. The light grey to buff to pink coloured diffuse overprint is advanced argillic 3 alunite alteration, which contains no significant associated sulfide (sample location Ogmaesan •*036*, 0.03ppm Au, <0.5ppm Ag; scale bar = 2cm). '**B**': Au-Ag mineralisation comprising dickite+pyrite±argentite infill associated with advanced argillic 2 alteration within the Seongsan system. Au-Ag mineralisation where present includes both disseminated dickite+pyrite±argentite as alteration and localised occurrences of vein-style mineralisation (SS001 186.35m, 1.59ppm Au, 8.6ppm Ag; scale bar = 2cm).

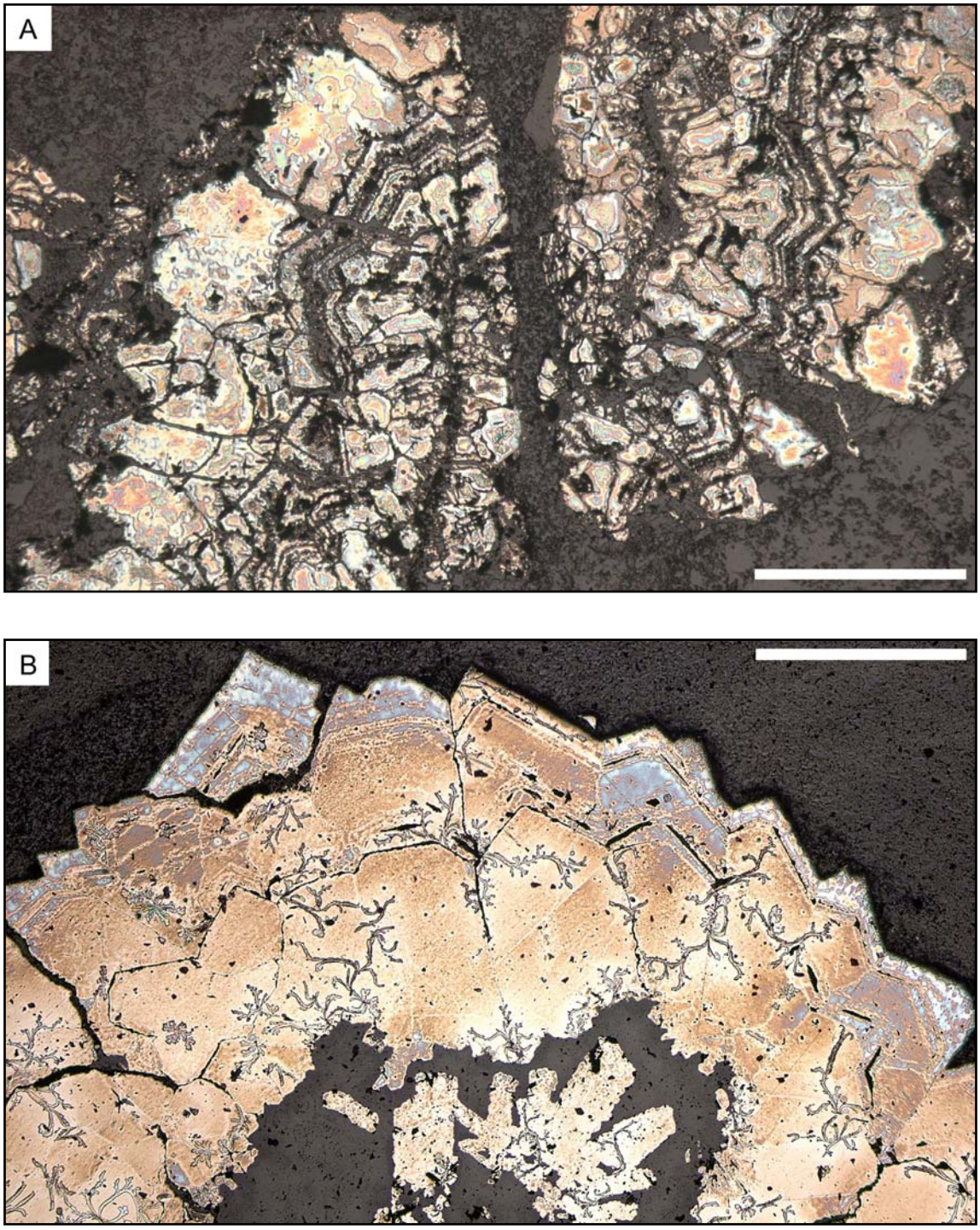

Fig. 3-4 Reflected light thin sections showing pyrite mineralisation associated with advanced argillic 2 alteration in a groundmass predominantly of quartz + dickite. '**A**': pyrite from Ogmaesan showing growth zones associated with varying As content (sample location Ogmaesan ●*016*, 0.05ppm Au, <0.5ppm Ag; scale bar = 0.5mm). '**B**': pyrite from Seongsan showing growth zones associated with varying As content (SS002 148.24m, 0.27ppm Au, 5.1ppm Ag; scale bar = 1mm).

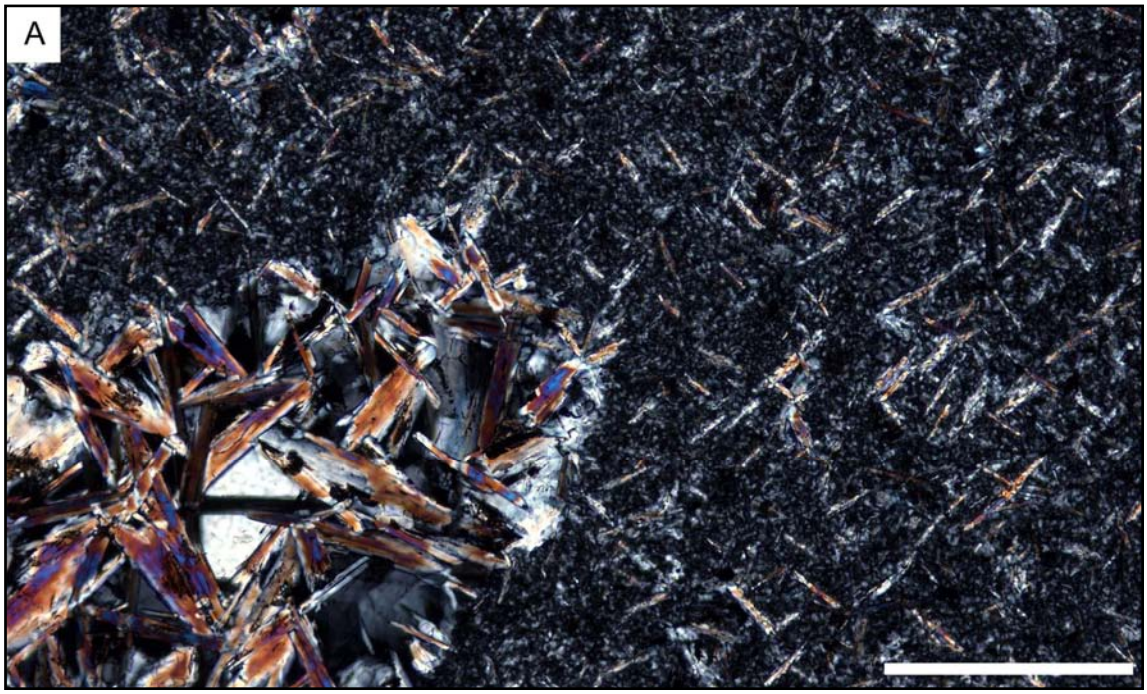

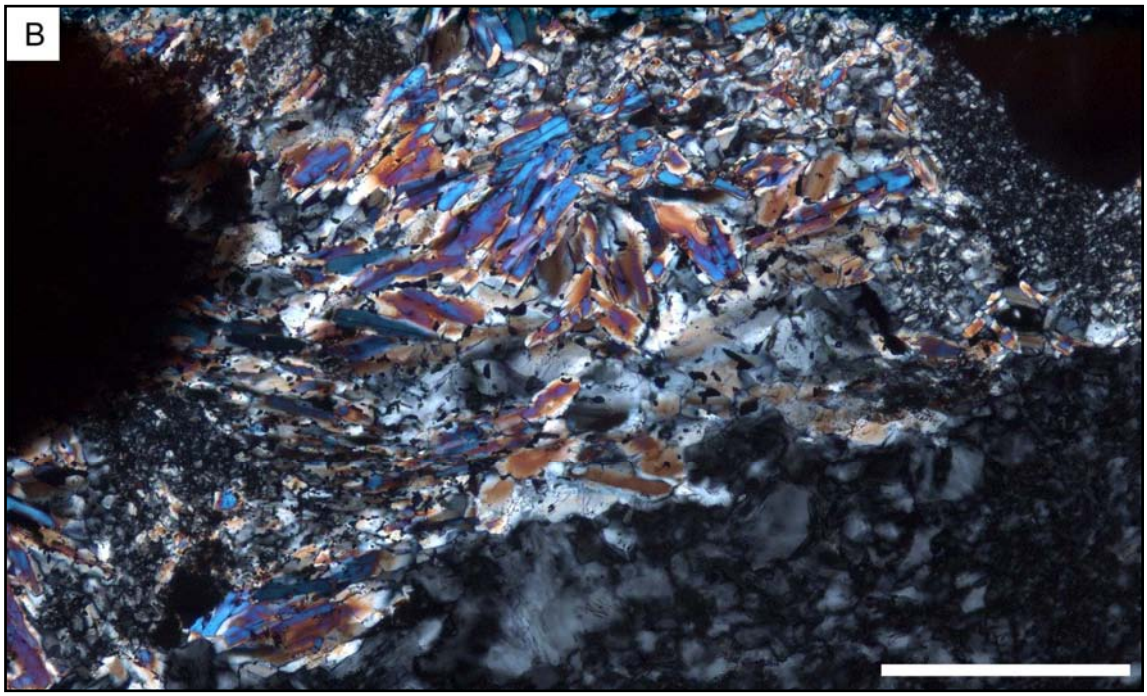

Fig. 3-5 Advanced argillic 3 alteration. '**A**': alunite occurring as coarse laths that replace phenocrysts and fine laths that replace matrix along with quartz and minor relic dickite (XPL, sample location Ogmaesan ●*059*, scale bar = 0.-25mm). '**B**': sample of ore material from the 'Alunite Pit' at Seongsan showing pervasive alunite+dickite alteration as alunite laths and coarse dickite. Dark material in the top left corner is black ink on the thin section (XPL, alunite ore; sample location ●*199*, scale bar = 0.25mm).

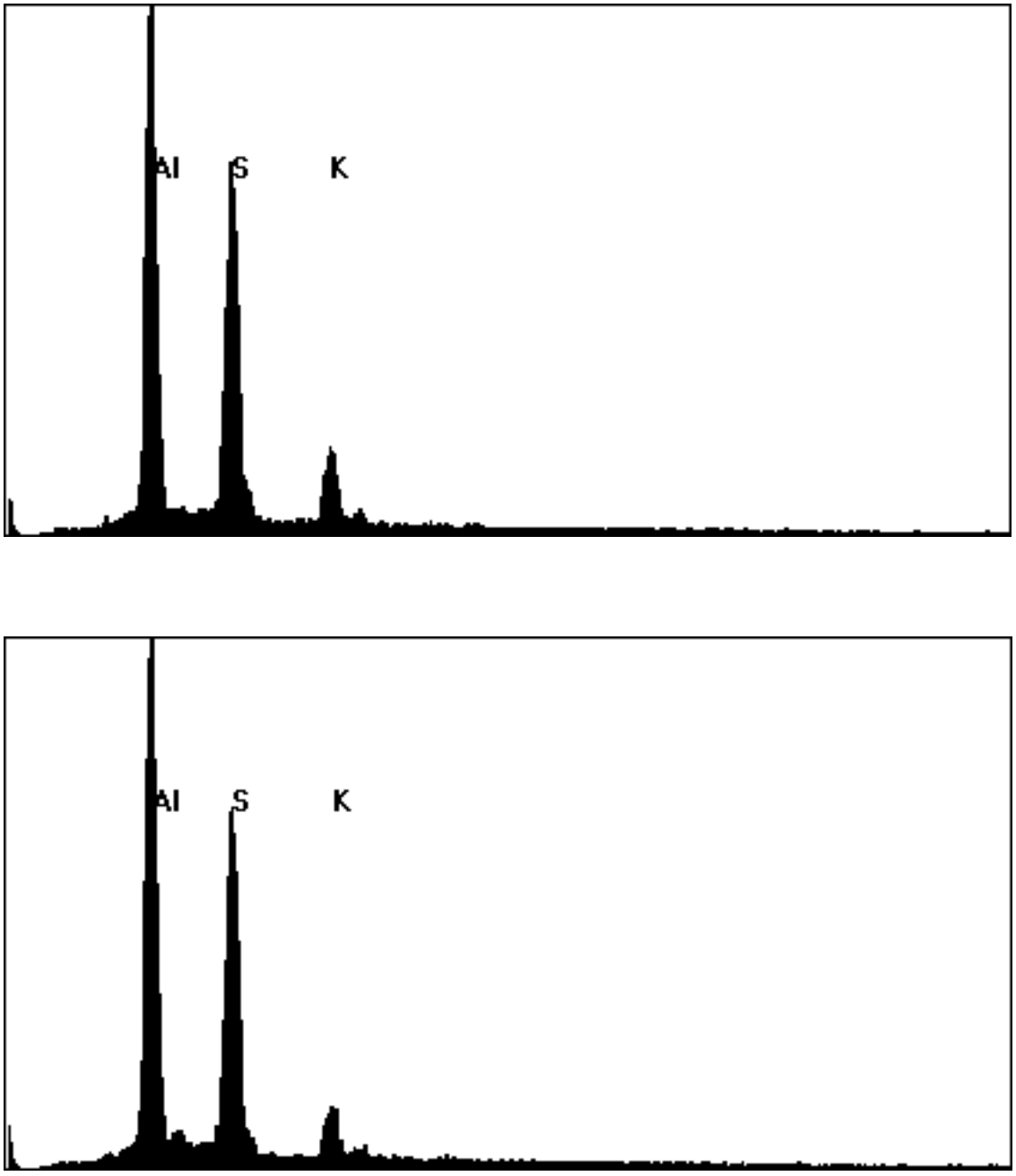

Fig. 3-6 EDS spectra from microprobe analyses of alunite from Seongsan (upper; sample SS 199) and Ogmaesan (lower; sample OG 59) showing their relatively simple K, Al and S composition (alunite = $KAl_3(SO_4)_2(OH)_6$).

The homogenous nature of alunites from the Seongsan district is distinct from other high sulfidation systems reported elsewhere, particularly so for Au-Ag±Au mineralised systems, which tend to show a wide variety of substitution within alunites associated with mineralisation (Hedenquist et al., 1994; Allibone et al., 1995; Deyell et al 2005). Oxygen, hydrogen and sulfur isotope analyses (Chapter 5) are conducted in an attempt to further constrain the conditions of formation during advanced argillic alteration.

3.2.6 Siliceous alteration

Siliceous alteration is recognised by the addition of silica to the rock with little or no clays (Fig. 3-7). Silicification is readily distinguished from other alteration types by its hardness due to silica flooding. Siliceous quartz develops as very fine-grained recrystallised stubby crystals typically inter-grown amongst relic quartz crystals and relic kaolinite±dickite±alunite±pyrite. Locally, siliceous alteration zones may host patchy silicic alteration as vuggy silica.

3.2.7 Silicic alteration

Silicic alteration comprises residual silica remaining after the loss of reactive components, resulting in a vuggy texture (Fig. 3-7). Silicic alteration can occur in a continuum from incipiently to intensely developed. Resulting silicic-altered zones therefore can show a continuum from patchy leaching, to zones where total reaction of reactive components has occurred leaving only massive residual silica.

3.2.8 Phyllic alteration

Phyllic alteration is characterised by the presence of illitic clay ±titanite/rutile(leucoxene) and pyrite and disseminated illite±pyrite in the rock matrix (Fig. 3-8). Phyllic-altered rocks in hand specimen typically contain visible disseminated pyrite and have a weakly bleached appearance. Where phyllic alteration is most strongly developed, albitised feldspar, carbonate-altered albitised feldspar, biotite and selective interstitial groundmass material are largely replaced by illitic clays.

Microprobe analyses show that phyllic alteration clays within the Seongsan district straddle the illite and phengite series solid solutions comprising end members muscovite and celadonite (Rieder, et al., 1998) (Fig. 3-9). The coarse illitic pseudomorphs of biotite, illitic replacement of carbonate-altered albitised feldspar and interstitial illitic clays have similar compositions despite their contrasting textures (Fig. 3-9). The fine interstitial micas tend to have a higher ratio of total interlayer cations and tend to plot slightly into the phengite series. By comparison, the coarser micas that replace biotite tend to have a lower ratio of total interlayer cations and tend to plot slightly into the illite series (Fig. 3-9).

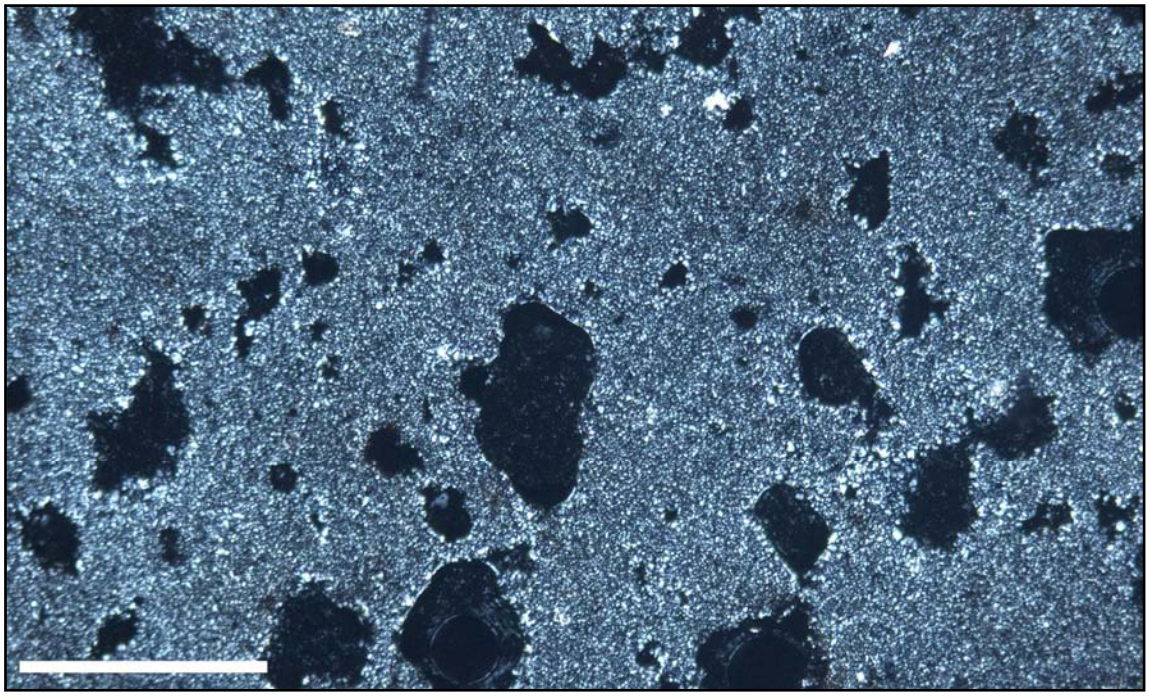

Fig. 3-7 Siliceous ± silicic alteration in thin section. The sample comprises texturally destructive silicification with minor leaching resulting in the development of vughs in the siliceous-altered rock. The vughs are presumed to be relic phenocryst sites that nucleated leaching. No evidence is preserved which would show whether leaching occurred of primary clay-altered or silicified phenocrysts. (XPL, sample location Ogmaesan ●*050*, scale bar = 0.5mm).

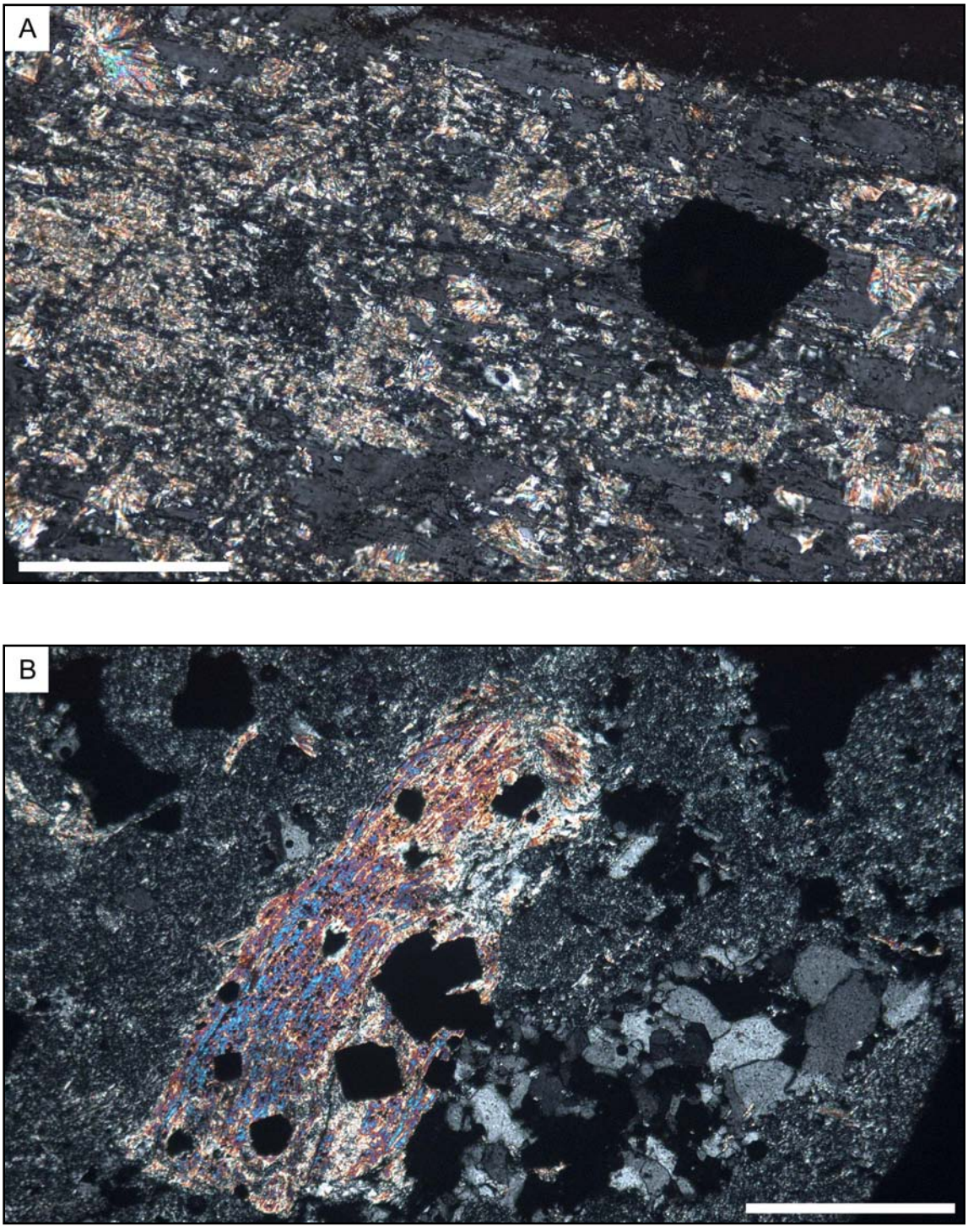

Fig. 3-8 Phyllic alteration in thin section. '**A**': medium-grained illitic clay replacement of albitised relic feldspar altered during the propylitic stage (XPL, EN004 68.5m, scale bar = 0.25mm). '**B**': coarse-grained illitic clay (illite+titanite/rutile(leucoxene)+pyrite) replacement of a biotite phenocryst (centre) plus fine-grained illitic clay replacement of the rock groundmass (XPL, MS013 118m, scale bar = 0.5mm).

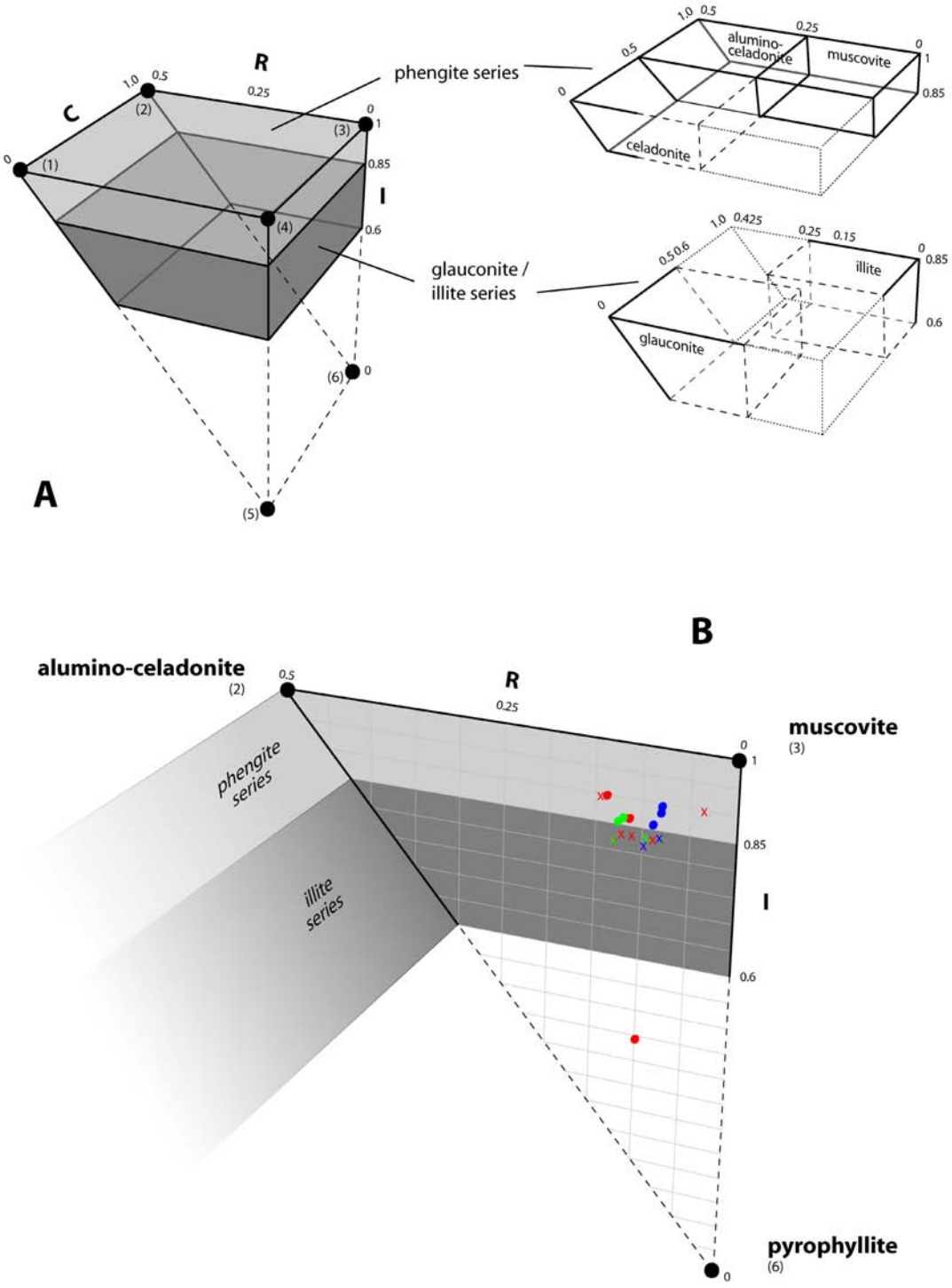

Fig. 3-9 '**A**': chemographic volume plot illustrating the relationship of some true dioctahedral micas (phengite series) to interlayer-cation-deficient dioctahedral micas (glauconite / illite series) (adapted from Rieder, et al., 1998). 'C' axis = ^{vi}Al / (^{vi}Al + $^{vi}Fe^{3+}$); 'R' axis = $^{vi}R^{2+}$ / ($^{vi}R^{2+}$ + $^{vi}R^{3+}$) - where '^{vi}' refers to the octahedral cations; 'I' axis = total interlayer cations. Solid dots refer to end-member micas as **(1)**: celadonite [$KFe^{3+}Mg\square Si_4O_{10}(OH)_2$], **(2)**: alumino-celadonite [$KAlMg\square Si_4O_{10}(OH)_2$], **(3)**: muscovite [$KAl_2\square AlSi_3O_{10}(OH)_2$], **(4)**: [$KFe_2^{3+}\square AlSi_3O_{10}(OH)_2$], **(5)**: [$\square Fe_2^{3+}\square Si_4O_{10}(OH)_2$] and **(6)**: pyrophyllite [$\square Al_2\square Si_4O_{10}(OH)_2$] – where '□' refers to a vacancy. Two blow-out slabs show the phengite series and the glauconite/illite series in further detail. Most dioctahedral micas from epithermal systems plot within the plane (2), (3), (6) as shown in 'B'. '**B**': Seongsan district phyllic alteration micas plotted on the alumino-celadonite – muscovite – pyrophyllite plane as determined from microprobe analyses. Fine interstitial micas (solid dots); coarse phenocryst replacement micas (crosses). Eunsan phyllic micas (n=5; green data), Moisan phyllic micas (n=9; red data) and Chunsan phyllic micas (n=5; blue data). See main text for discussion; see Appendix 2 for sample list.

3.2.9 Adularia alteration

Adularia alteration is characterised by the presence of adularia, typically as overgrowths on relic albitised feldspar (Fig. 3-10). Microprobe analyses of adularia confirmed the chemical composition as end-member K-feldspar composition (Fig. 3-11) as distinct from igneous K-feldspar which tends to contain greater albite and anorthite components. Adularia is usually defined as a morphologically distinctive variety of potassium feldspar, typically as a partially ordered low-temperature polymorph of orthoclase, ($KAlSi_3O_8$) (Smith, 1974; Černý & Chapman, 1986).

Adularia alteration is difficult to identify in hand specimen, but is recognised in thin section by the distinct texture of overgrowths on earlier albitised (±phyllic altered) feldspars (Fig. 3-10). Adularia also occurs as infill material in veins and is typically associated with Au (see: Section 3.3.5). The development of alteration and infill adularia appear to be closely associated.

Phyllic and adularia alteration show a more subtle zoning compared with the generally more pervasive and texturally destructive advanced argillic alteration. In phyllic- and adularia-altered zones, relict minerals associated with propylitic and phyllic alteration assemblage often occur in the same specimen. Feldspars show the most variation in terms of overprinting minerals and have been used to define the extents of assemblages, i.e. the recognition of adularia rims on albitised feldspars marks the transition of the adularia zone.

3.2.10 Carbonate (late-stage) alteration

Late-stage carbonate alteration is characterised by the presence of carbonate as replacement of phenocrysts and/or groundmass. Late-stage carbonate alteration is distinguished from propylitic carbonate alteration at outcrop scale by its spatial association with discordant late-stage carbonate veins, which cut phyllic, advanced argillic and propylitic alteration (see: Section 3.3.3).

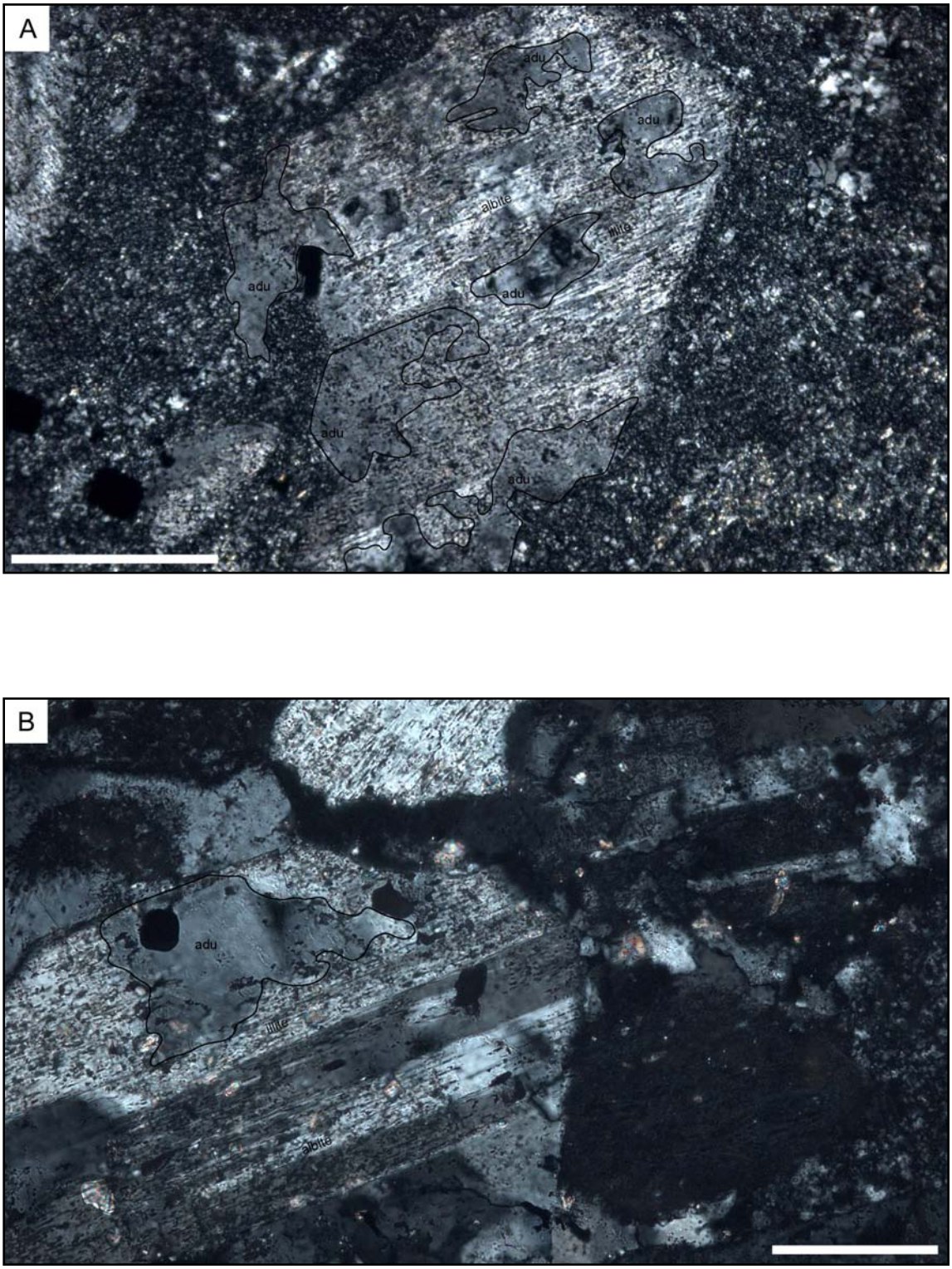

Fig. 3-10 Adularia alteration in thin section. '**A**': phyllic-altered albitised feldspar partially replaced by illite and then overprinted by adularia, which forms clear grey irregular patches that lack illite (EN004 133m, scale bar 0.25mm). '**B**': phyllic-altered albitised feldspar partially replaced by illite and then overprinted by adularia, which forms clear grey irregular patches that lack illite (MS001 186.5m, scale bar = 0.1mm).

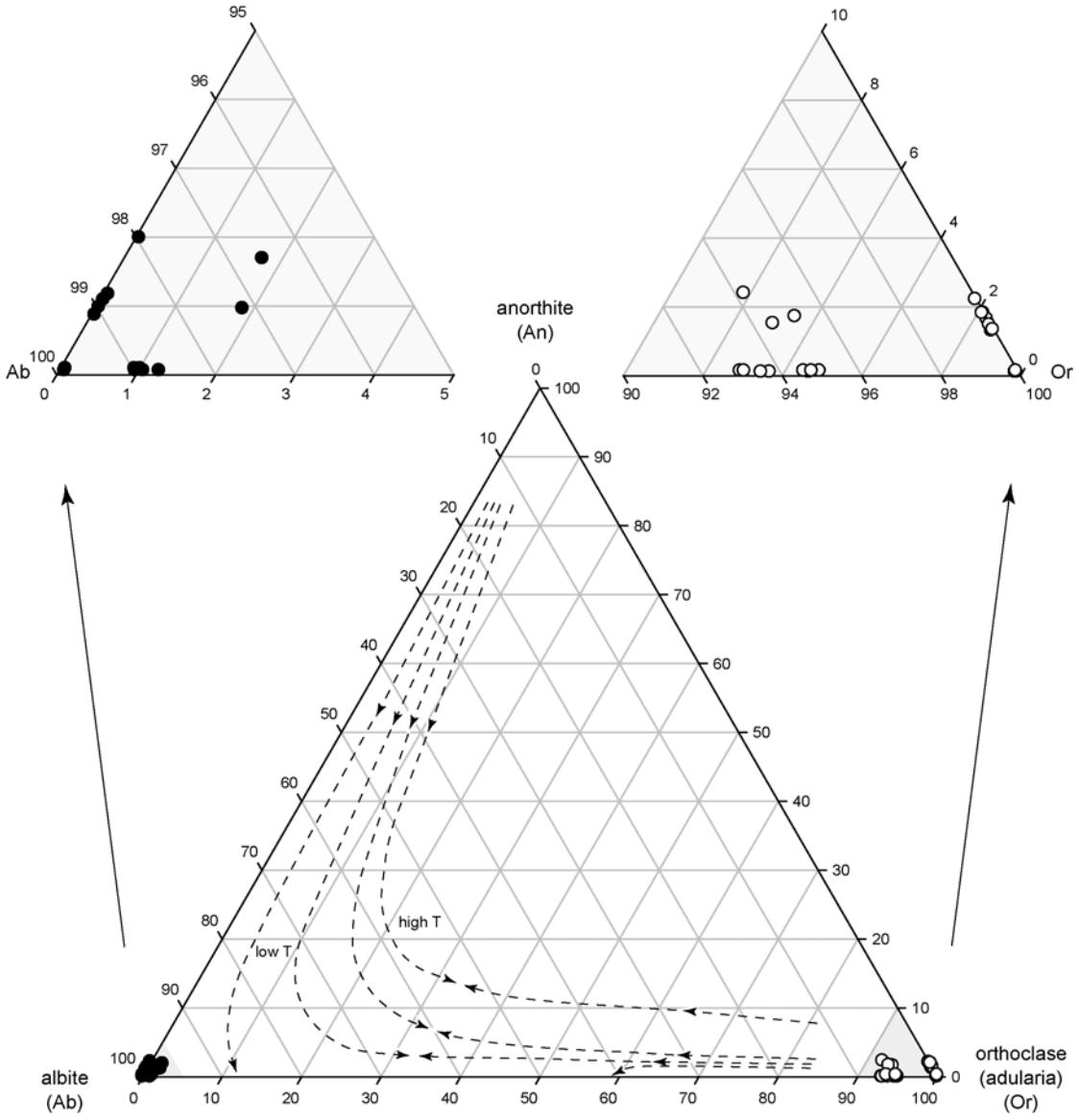

Fig. 3-11 Ternary plot showing the composition of feldspars associated with propylitic alteration (solid dots) and feldspar overgrowths during adularia alteration (open dots) from the Seongsan district. Grey shaded areas show detailed sections of the data from the main ternary plot. Propylitic altered feldspars range from $Ab_{96.7}Or_{1.7}An_{1.6}$ to Ab_{100} (Eunsan and Moisan; n=21), adularia altered feldspars range from $Or_{92.0}Ab_{5.7}An_{2.3}$ to Or_{100} (Eunsan, Moisan and Chunsan; n=84). No primary unaltered feldspars were found in the Seongsan district, but reaction pathways for feldspars forming from fluids of different initial temperatures are shown by the dashed lines with arrows indicating direction of cooling temperature (from Tuttle & Bowen, 1958). These pathways highlight that end-members orthoclase and albite are highly unlikely primary products. Their presence within the Seongsan district is evidence for hydrothermal alteration and highlights the distinctly different compositions of feldspars from the respective alteration assemblages. See Appendix 2 for sample list and raw data.

3.3 VEINING AND INFILL MATERIAL

Vein assemblages and infill material are listed in Table 3-2 and can be broadly separated into either clay-sulfide, quartz-dominated or carbonate-only assemblages.

3.3.1 Clay-sulfide vein/infill assemblages – associated with advanced argillic alteration

Clay-sulfide veining and infill are generally restricted to the Seongsan and Ogmaesan systems, with minor occurrences at Chunsan. Clay-sulfide veining and infill material comprise veins generally 1 to 3cm wide, but locally up to 10cm wide, of massive to crystalline dickite/kaolinite and pyrite (Fig. 3-3). Typically these veins have irregular shapes and poor lateral continuity. They sometimes form as networks of veins. Veins often show discordant crosscutting relationships to bedding, highlighting their infill nature (Fig. 3-3). Locally, distinguishing clay-sulfide infill from clay-sulfide alteration can be difficult, particularly when clay-sulfide veins show a close spatial association with clay-sulfide alteration. Texturally they can appear very similar due to the texture destructive nature of advanced argillic clay-pyrite alteration. In addition to veining, clay-sulfide infill also forms infill breccia matrix. Breccia matrix material is generally rich in sulfide, although locally breccias contain significant kaolinite/dickite.

Infill sulfide mineralisation is dominated by pyrite. Ag-sulfides (argentite/acanthite Ag_2S), electrum, Fe-poor sphalerite and galena have also been recognised locally. Au-Ag and base metal mineralisation is typically not present beyond grades of 0.2ppm. Where Au-Ag mineralisation is present, it occurs as inclusions in pyrite.

Clay-sulfide infill assemblages and clay-sulfide alteration assemblages developed during advanced argillic 1 and 2 alteration are essentially the same. Both are also closely associated spatially. The relationship between clay-sulfide veins and clay-sulfide alteration is interesting. As there is more clay-sulfide alteration than can be reasonably explained by the relatively small volume of clay-sulfide veining observed, assuming that the clay-sulfide veins were conduits for hydrothermal fluids responsible for clay-sulfide alteration seems highly unlikely. This implies that grain boundary diffusion was an important process. Alternatively, the clay-sulfide veins may have been derived from a closed system reorganisation of pre-existing clay-sulfide pervasively altered wall-rocks (Oliver & Bons, 2001).

Vein assemblages	Infill material	Infill forms	Associated metals^
clay-sulfide	py+dick/kao±argentite±electrum± Fe-poor sphalerite±galena	massive, crystalline	Au, Ag, Pb, Zn
qtz±carb	qtz±carb	crystalline, chalcedonic banded	generally none
qtz±adularia±sulfide ±metal	qtz±adularia±py±Ag-sulfides ±Ag-sulfo salts±cpy±Fe-poor sph±galena±ten/tet±tell± electrum±native Ag± native Te	crystalline, banded, colloform, crustiform, cockade, rhombic(adu), tabular(adu), acicular(adu)	Au, Ag, Cu, Pb, Zn, Te
carb-only	carb	bladed, massive, crystalline	none

Table 3-2 A broad classification of vein assemblages, infill material, infill forms and associated metals within the Seongsan district. See text for further detail. Individual systems show some localised variations as discussed within Section 3.4. ^ - associated metals are not always present. py = pyrite; dick = dickite; kao = kaolinite; qtz = quartz; carb = carbonate; adu = adularia; cpy = chalcopyrite; sph = sphalerite; ten/tet = tennantite/tetrahedrite; tell = tellurides

3.3.2 Quartz-dominated vein assemblages

Numerous quartz-dominated vein assemblages are present at Eunsan and Moisan, with only minor occurrences at Chunsan and Seongsan. Individual veins typically contain a wide variety of textures and mineralogy. The most common vein assemblages and textures are listed in Table 3-2. This section gives an overview of the main quartz-dominant vein assemblages within the Seongsan district. The paragenesis of these veins is discussed in detail in Sections 3.4 and 3.5.

3.3.2.1 Quartz± carbonate vein assemblages

Quartz only veins are dominated by either crystalline or chalcedonic quartz. Crystalline quartz veinlets are 1 to 10mm wide, often contain a central void, and are generally restricted to shallow levels. Chalcedonic quartz veins are 1 to 3cm wide and are also generally restricted to shallow levels. Quartz-carbonate only veins are uncommon, but where present are characterised by intergrown crystalline quartz and carbonate.

3.3.2.2 Quartz± adularia± sulfide± metal vein assemblages

These are the most significant Au-Ag bearing veins in the Seongsan district. A wide variety of vein assemblages are present that include quartz±adularia±sulfide±metal. Some veins are dominated by quartz-adularia with relatively minor sulfide, whereas others are dominated by sulfide with only minor quartz-adularia. The presence of colloform banded textures and adularia distinguishes these sulfide-rich veins from sulfide-rich, clay-bearing veins associated with advanced argillic alteration described previously. Additionally, carbonate can form within these veins, typically as late infill. These veins show a broad range of textures (Section 3.3.4) and can develop either as discrete veins or as vein breccias. Quartz-adularia rich veins are associated with the adularia alteration described in Section 3.2.9.

Sulfides and metals observed within these veins include: pyrite, Ag-sulfides, Ag-sulfo salts, Fe-poor sphalerite, galena, chalcopyrite, goldfieldite-tennantite/tetrahedrite, Au-Ag rich tellurides, electrum, native Ag and native Te. These are discussed further with respect to each prospect in Section 3.4.

3.3.3 Carbonate-only vein assemblage

Two types of carbonate-only veins are present. Early-stage bladed carbonate veins and late-stage massive to crystalline carbonate veins. The early-stage bladed carbonate veins are not common, whereas late-stage carbonate veins are commonly found discordantly overprinting the main stages of mineralisation and adularia, phyllic, advanced argillic and propylitic alteration.

These late-stage carbonate veins show a close spatial affinity to the development of late-stage carbonate alteration (see: Section 3.2.10).

3.3.4 Quartz textures and vertical zonation

Examination of numerous quartz vein samples from surface and diamond drill core from Eunsan and Moisan shows that vein quartz textures and mineralogy for given stages of quartz development (discussed further in Section 3.4.2.2) show a distinct vertical zonation (Fig. 3-12). A vertical zonation of vein quartz textures and mineralogy in epithermal vein systems has been well documented previously by Morrison et al. (1990) and Dong et al. (1995).

Quartz textures include: saccharoidal to drusy quartz; replacement of bladed carbonate by quartz; crystalline to mesocrystalline banded quartz(±adularia) veins; cockade to colloform banded quartz veins; diffuse black silica; chalcedonic quartz; and amorphous silica flooding. At Eunsan and Moisan, quartz veins show a vertical zonation of both texture and mineralogy, although some degree of overlap between textural zones occurs, especially at Moisan. Generally, upper zones comprise saccharoidal, drusy and chalcedonic quartz, progressively passing through a central zone of quartz after bladed carbonate to colloform and crustiform quartz and into a lower zone of crystalline quartz (Fig. 3-12). Mineralogical zoning is schematically illustrated in Figure 3-12.

3.3.5 Adularia textures

Adularia vein infill is much less widespread than quartz vein infill, except at Chunsan where significant adularia infill has occurred (Section 3.4.2.2, pg 3-32). Adularia growths can be classified as: sub-rhombic, rhombic, tabular, and pseudo-acicular (Dong & Morrison, 1995). Where vein infill adularia is present, adularia develops predominantly as rhombic and sub-rhombic material with lesser amounts of tabular material, all typically associated with quartz. Generally the grain size of these adularia crystals are in the order of 0.2 to 1.5mm, <0.1mm and <1 to 2mm in length respectively.

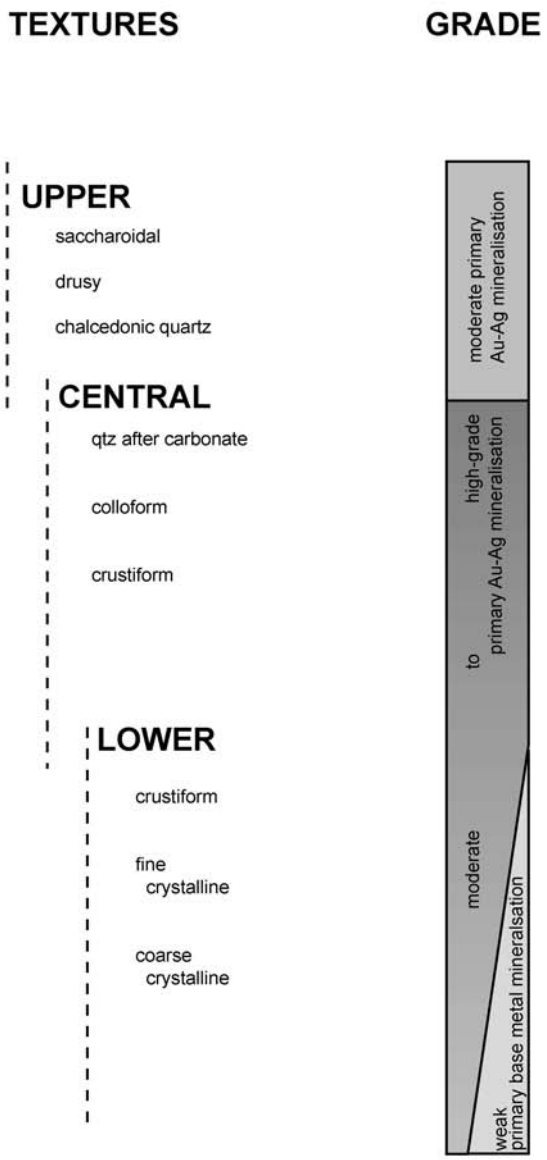

Fig. 3-12 Semi-schematic diagram based on numerous observations from Eunsan and Moisan illustrating the vertical zonation of vein quartz textures with associated approximate primary Au±Ag and base-metal grade relationships.

3.3.6 Composition of carbonates

Microprobe analyses of propylitic alteration replacement carbonates, early- to syn-mineral vein carbonates and late-stage carbonate veins are plotted in Figure 3-13. See Appendix 2 for sample list.

Eunsan carbonates are all nearly pure calcite, with less than 0.07 mol fraction substitution by Mn and less than 0.02 mol fraction substitution by Mg and Fe. Propylitic alteration carbonates (n=3) are calcite with minor Mn substitution. Early- to syn-mineral vein carbonates (n=10) includes both pure calcite and Mn-calcite. Late-stage carbonate veining (n=17) are also calcites with minor Mn and Mg substitution.

Chunsan carbonates are all nearly pure calcite, with less than 0.07 mol fraction substitution by Mn and less than 0.02 mol fraction substitution by Mg and Fe. Propylitic alteration carbonates (n=2) are calcite with trace Fe substitution. Early- to syn-mineral vein carbonates (n=3) are pure calcite. Late-stage carbonate veining (n=9) are calcites with minor Mn and Mg substitution.

Moisan carbonates are relatively pure calcite, with up to 0.36 mol fraction substitution by Mg and up to 0.32 mol fraction substitution by Mn, with less than 0.05 mol fraction substitution by Fe. Propylitic alteration carbonates (n=6) show significant Mn impurities present with minor Mg and trace Fe substitution. Early- to syn-mineral vein carbonates (n=8) show the most deviation from pure calcite as Mn-calcite and Mg-calcite with trace Fe substitution in both. Late-stage carbonate veining (n=7) are Mn-calcites. Moisan carbonates show a much broader chemical compositional range compared to those at Eunsan and Chunsan, despite carbonate development being less extensive at Moisan compared to Eunsan.

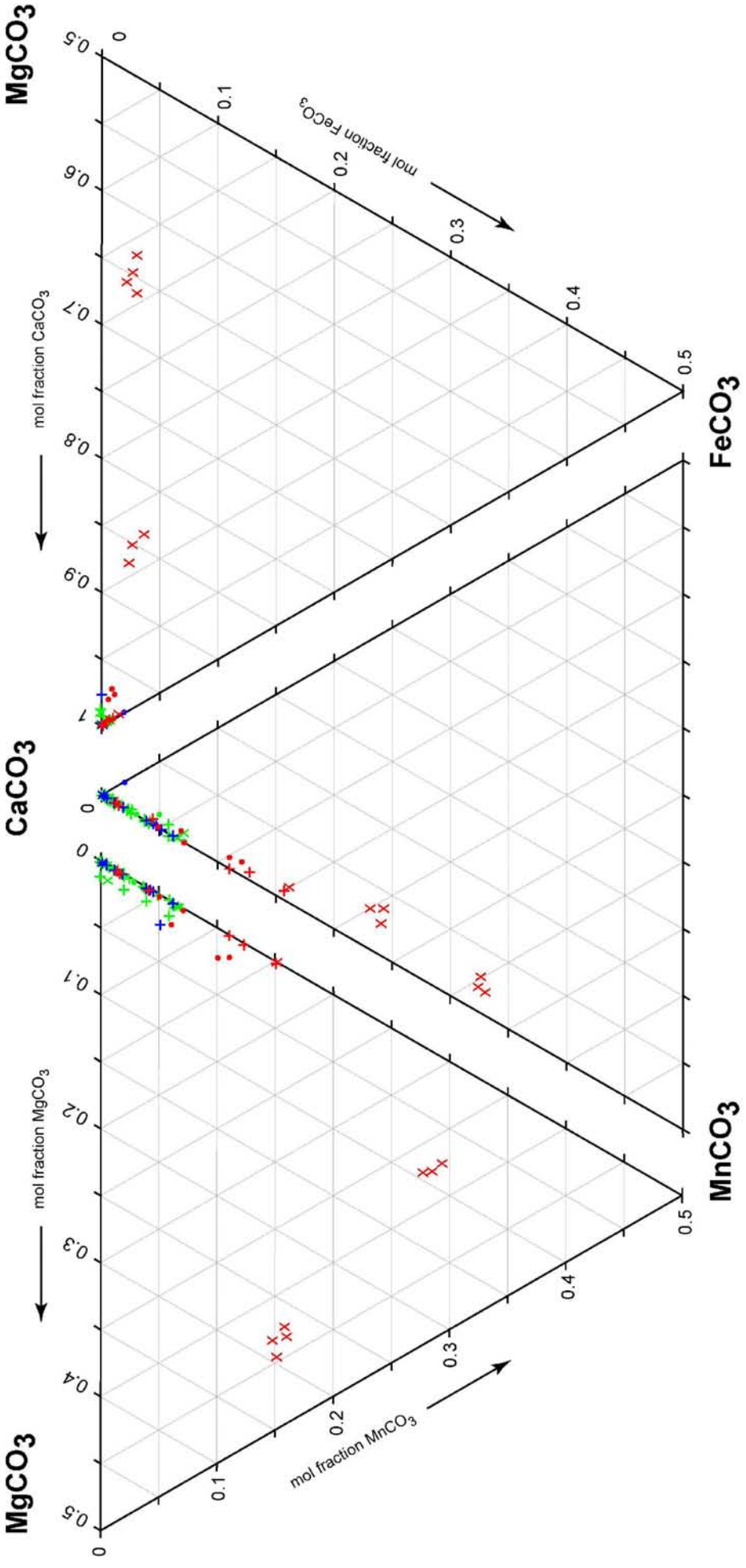

Fig. 3-13 Exploded view of microprobe data for various carbonates from the Seongsan district, projected onto the faces of the $CaCO_3$ tip of the $CaCO_3$ – $MgCO_3$ – $MnCO_3$ – $FeCO_3$ tetrahedron. Data represents propylitic alteration carbonates (n=11; solid dots), vein carbonates (n=21; crosses) and post mineral carbonates (n=33; pluses); green data for Eunsan, red data for Moisan and blue data for Chunsan. Individual ternary plots were generated by normalising data for the given ternary system resulting in equivalent representation of projected quaternary data. See main text for discussion (pg 3-22 to 3-24).

3.4 PARAGENESIS

It is important to examine the processes by which alteration occurs to better understand the implications of overprinting alteration assemblages. This understanding is critical to our interpretation of alteration assemblages forming over time and space.

3.4.1 Overprinting alteration assemblages: development over time or space …?

A variety of different alteration assemblages characterise many hydrothermal systems (Reed, 1997). Different alteration assemblages are commonly confined to discrete zones within the broader volume of altered rock. A variety of overprinting relationships are often developed along the margins of these zones where different alteration assemblages are in contact with each other (Reed, 1997), a common feature in the hydrothermal system of the Seongsan district.

Alteration overprinting relationships and zonation develop either from distinctly different fluids overprinting previously existing alteration (e.g. advanced argillic overprinting propylitic) or in response to advancing chemical and thermal mineral stability fronts (e.g. the zoning from peripheral advanced argillic 1 alteration to core advanced argillic 3 zones) (Korzhinskii, 1965).

Alteration assemblages developed from distinctively different fluids form at different times. An example of this is propylitic alteration overprinted by younger advanced argillic alteration, typical of many acid-sulfate systems. Under this situation, overprinting relationships do reflect changes in fluid chemistry over time (Reed, 1997).

Alteration assemblages developed from advancing alteration fronts form at essentially the same time. An example of this is the various concentrically zoned advanced argillic assemblages in many acid-sulfate systems (e.g. Temora, Allibone et al., 1995). Under this situation, overprinting relationships develop at alteration fronts where advancing alteration has yet to completely destroy one or more previous assemblages. Alteration assemblages will differ depending on their distance from primary hydrothermal fluid ascent zones. This does not reflect a change in the chemistry of the hydrothermal fluid over time, but rather the lower fluid to rock ratios and increasingly rock-buffered fluid chemistry more distant from the primary ascent zone and/or thermal chemical stability fronts from core zones to peripheral zones. Alteration fronts could continue to advance for the life of the hydrothermal system, or until fluid-rock equilibrium is reached at the system margins.

Developing an understanding of the overprinting relationships and their temporal significance is a key stage in constraining the chemical and thermal evolution of a hydrothermal system. Once

the alteration and mineral paragenesis is understood, fluid inclusion and isotope data derived from altered rocks can be placed in their broader temporal and chemical context.

3.4.2 Paragenetic events within the Seongsan district

Propylitic alteration is the earliest alteration recognised. Relic albitised±carbonate-altered feldspars and illitic-altered biotite phenocrysts remain in the most peripheral parts of several epithermal systems of the Seongsan district (Section 3.2.1; Fig. 3-1). Each epithermal system in the Seongsan district is superimposed on the propylitic alteration.

Within the epithermal systems, two distinct paragenetic sequences of assemblages are developed.

1. systems that are dominated by hypogene advanced argillic alteration, or
2. systems that are dominated by phyllic-adularia alteration development.

The series of paragenetic events in each system is summarised in Table 3-3 (pg 3-48) after they have been described. This table highlights the similarities and differences between each of the systems.

Systems that are dominated by hypogene advanced argillic alteration are represented by Seongsan and Ogmaesan and discussed in Section 3.4.2.1. Eunsan and Moisan show dominantly phyllic-adularia alteration and are discussed within Section 3.4.2.2. They show evidence for having undergone hypogene advanced argillic alteration, although this is limited to incipient peripheral affects. Chunsan has undergone significant hypogene advanced argillic alteration and phyllic-adularia alteration. Chunsan is therefore discussed within both Sections 3.4.2.1 and 3.4.2.2.

3.4.2.1 Paragenetic events in systems that are dominated by hypogene advanced argillic alteration

The alteration zonation in the hypogene advanced argillic alteration systems Seongsan, Ogmaesan and Chunsan are described below, in sequence from peripheral to core zones (Figs. 3-26, 3-27, 3-30).

Advanced argillic 1 alteration

The most peripheral alteration assemblage observed within these systems is advanced argillic 1 alteration. The transition from propylitic alteration to advanced argillic 1 alteration has not been observed as outcrops and available diamond drill core do not extend far enough out of these

systems to intersect this transition. Within the advanced argillic 1 zone, both feldspars and biotite phenocrysts are completely replaced by kaolinite. The rock matrix has been pervasively altered to kaolinite±quartz (Table 3-3). Mineralogically similar but only incipient advanced argillic 1 alteration is developed at Eunsan and Moisan.

Advanced argillic 2 alteration ± Au-Ag mineralisation

Advanced argillic 2 alteration is developed closer to the core of each system. The transition from advanced argillic 1 to advanced argillic 2 alteration assemblages is marked by an increase in the amount of dickite, with a decrease in the amount of kaolinite (Table 3-3). Since dickite is a higher temperature polymorph of kaolinite, the change from kaolinite to dickite is interpreted to represent a thermal mineral stability boundary with increasing temperature closer to the core of each system.

Clay-sulfide veining and infill ±Au-Ag mineralisation developed synchronously with the development of advanced argillic 2 alteration (Table 3-3; Section 3.3.1). At Seongsan, zones of quartz±dickite±pyrite±argentite-altered and mineralised rock often contain up to 2ppm Au and 15ppm Ag. Peak assays for Au are 12.90ppm and 92ppm for Ag. At Ogmaesan, localised zones of clay-sulfide veining and infill are barren with respect to Au-Ag mineralisation.

Advanced argillic 3 alteration

Advanced argillic 3 alteration is developed closer again to the core of each system. The transition from advanced argillic 2 to advanced argillic 3 alteration assemblages is marked by an increase in the amount of alunite, with a decrease in the amount of dickite (Table 3-3). The formation of alunite requires relatively high SO_4^{2-} activity, hence the change from alunite to dickite represents a chemical stability boundary. Where SO_4^{2-} activity has diminished sufficiently, a change in mineral stability from advanced argillic 3 alunite to advanced argillic 2 dickite is inferred to have occurred. Phase diagrams that allow an interpretation of these mineralogical changes are presented within Chapter 5. At Chunsan, advanced argillic 3 alteration assemblage has not developed extensively.

Siliceous ± silicic alteration

Core zones show siliceous and/or silicic alteration development, characterised by texturally destructive replacement by silica and/or leaching (Table 3-3). Zones of intense siliceous and/or silicic alteration development at Seongsan are typically associated with sub-economic Au grades of <0.50ppm. Chunsan locally shows the most significant vuggy silica development within the Seongsan district. The widespread lack of an advanced argillic 3 zone between the

advanced argillic 2 and silicic zones at Chunsan implies a different fluid evolution to the Seongsan and Ogmaesan systems.

Overprinting phyllic±adularia±carbonate alteration and/or quartz veins

Phyllic±adularia±carbonate alteration and/or quartz±adularia-veins cut the advanced argillic alteration at Seongsan, Eunsan, Moisan and Chunsan.

At Seongsan, overprinting carbonate and phyllic alteration both overprint and partly destroy earlier advanced argillic alteration assemblages (Fig. 3-14). Based on textural and mineralogical similarities, the carbonate and phyllic alteration within the Seongsan system (Fig. 3-14) are most likely associated with nearby discordant quartz-veins located approximately 100m away (SS002 134.9m and Seongsan Clay Mining Co. DDH 87-1 92.8m) (Fig. 3-15). Petrographic analyses indicate that the illitic clays are similar to those at Eunsan, Moisan and Chunsan. All are illite/phengite series clays that form part of a solid solution between muscovite-celadonite (Fig. 3-9).

These field relationships indicate that carbonate and phyllic alteration and associated quartz-veining both post-date advanced argillic alteration. However, it is not clear whether they pre- or post-date, or developed synchronously with the late-stage normal faulting that cross-cuts the advanced argillic alteration (Chapter 2, Section 2.3.3.1; Fig. 2-25).

3.4.2.2 Paragenetic events in systems that are dominated by phyllic-adularia alteration

The alteration zonation in the phyllic-adularia alteration systems Eunsan, Moisan and Chunsan are described below, in sequence from peripheral to core zones (Figs. 3-28 to 3-30).

Phyllic alteration ± early carbonate veining

Phyllic alteration overprints propylitic alteration (Figs. 3-28 and 3-29) and also overprints advanced argillic 1 alteration where present (Fig. 3-14; Table 3-3). The illitic clays associated with phyllic alteration overprint albitised and carbonate-replaced feldspar phenocrysts and clay altered biotite phenocrysts previously affected by the propylitic alteration (Fig. 3-8). Illitic clays, quartz and pyrite associated with the phyllic alteration assemblage also replace the rock matrix. When in contact with advanced argillic assemblages, the same illitic clays overprint kaolinite±dickite clays, particularly when accompanied by crosscutting carbonate veinlets (Fig. 3-14). Phyllic alteration forms peripheral zones broadly concentric with inner adularia zones, although the boundary between phyllic alteration and inner adularia zones tends to be diffuse.

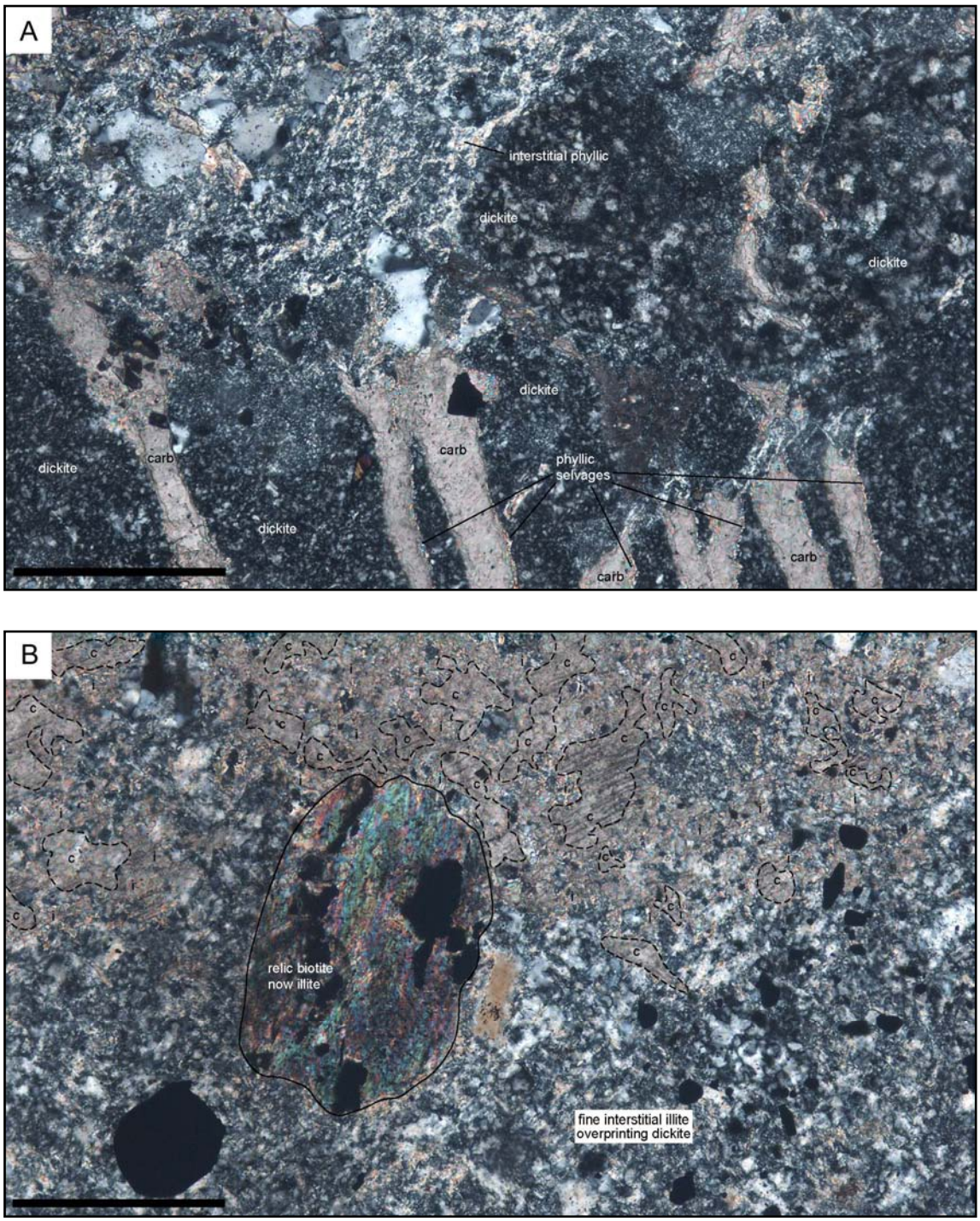

Fig. 3-14 Rare carbonate and phyllic alteration overprinting dickite alteration at Seongsan. '**A**': carbonate veinlets with selvages of phyllic alteration and interstitial phyllic alteration; both overprinting earlier dickite alteration (sample SS001 298.5m, scale bar = 0.25mm). '**B**': primary biotite phenocryst (centre) replaced by a mixture of coarse platy illite and leucoxene with fine interstitial illite (i) overprinting carbonate (c) (top half) leaving corroded but optically continuous patches of carbonate (note the parallel cleavage between patches); both carbonate and illite are associated with phyllic-carbonate alteration which overprints earlier dickite alteration (bottom half) (sample SS001 298.5m, scale bar = 0.25mm).

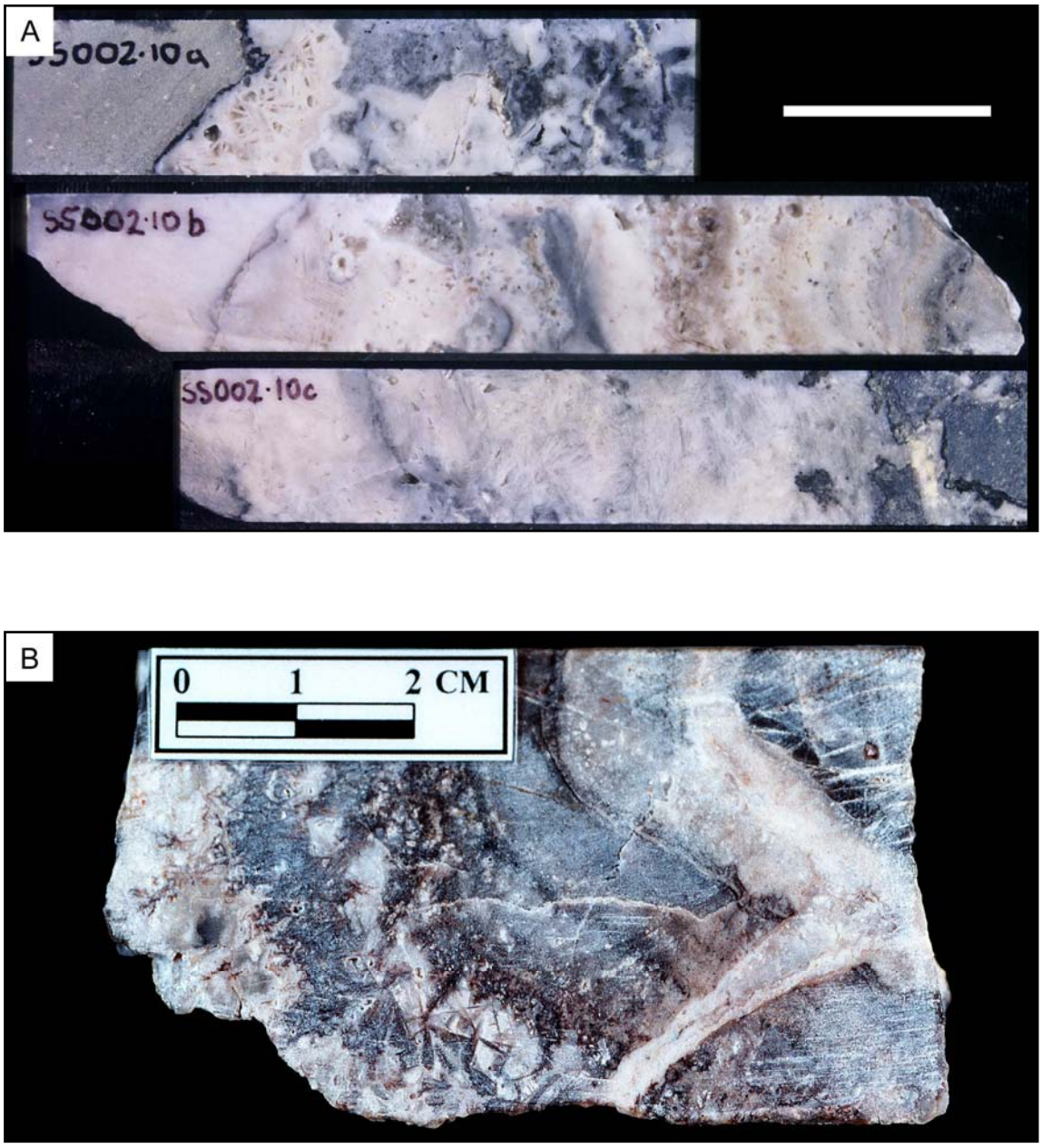

Fig. 3-15 Quartz veins within the Seongsan system that cut earlier advanced argillic alteration. '**A**': From SS002 (134.9m; scale bar = 3cm), continuous pieces of quartered HQ core totalling ca. 30cm of vein material that comprises pseudo-colloform to pseudo-crustiform banded quartz, quartz after bladed carbonate, massive chalcedonic quartz, comb quartz and minor saccharoidal quartz. Dark bands of sulfides in the interval 134.87m to 135.23m (0.36m) assayed 0.13ppm Au, 1.3ppm Ag. Host rock in the top left is strongly advanced argillic 2 altered. '**B**': From DDH 87-1 (Seongsan Clay Mining Co., 92.8m; photo courtesy of Ivanhoe Mines Ltd.), ca. 5cm of vein material comprised of pseudo-colloform banded quartz with bladed carbonate dissolution textures. The interval 92.8m to 93.8m (1m) re-assayed by Ivanhoe Mines Ltd. returned 0.41ppm Au, 3.9ppm Ag (Panther et al., 2000). These veins are similar in texture to mineralised veins in the phyllic-adularia alteration dominated Eunsan and Moisan systems implying similar but minor hydrothermal activity occurred within the Seongsan system late in the paragenesis.

Bladed carbonate veins are overprinted by adularia and siliceous alteration, which implies that they developed prior to or synchronous with phyllic alteration. Bladed carbonate veins are pseudomorphed by quartz, preserving the original bladed texture; blades typically range from 0.5 to 4cm long (Fig. 3-16). Occurrences of this stage of veining are restricted to shallow levels in the central and western parts of Eunsan and rare occurrences at Chunsan. Carbonate veins associated with phyllic alteration at Seongsan (Fig. 3-14) are inferred to be associated with this stage as they share similar cross cutting field relationships.

Adularia alteration at Eunsan, Moisan and Chunsan and disseminated quartz-adularia-sulfide-metal infill at Chunsan

Adularia alteration is developed peripheral to core siliceous zones at Eunsan, Moisan and Chunsan. The change from phyllic to adularia alteration is marked by a decrease in the amount of illite/phengite and the appearance of adularia, generally as overgrows on relic feldspar (Table 3-3). Where adularia alteration is strongly developed, such as at Eunsan, illitic clays and albitised feldspars are completely replaced by adularia (Fig. 3-10), resulting in adularia altered zones that are broadly concentric with core siliceous altered zones (Fig. 3-28). If only weakly developed, such as at Moisan, illitic clays and albitised feldspars are only partly replaced (Fig. 3-1), resulting in scattered discontinuous zones of adularia alteration surrounding core siliceous altered zones (Fig. 3-29).

Alteration at Chunsan is extensive and comprises both advanced argillic and phyllic-adularia alteration assemblages (Table 3-3). Figure 3-17 shows earlier advanced argillic rock at Chunsan, characterised by kaolinite-quartz advanced argillic 1 alteration and patchy leaching, progressively being overprinted by siliceous and adularia alteration and associated Au-Ag mineralisation. Where the adularia-Au-Ag mineralisation overprint is strongly developed, relic advanced argillic alteration is completely obliterated by quartz-adularia-sulfide-metal infill (Fig. 3-18). These field relationships clearly illustrate that phyllic-adularia alteration and associated Au-Ag mineralisation overprints earlier advanced argillic alteration.

Sulfide-metal assemblages associated with this stage of mineralisation commonly observed at Chunsan are pyrite (FeS_2) ± electrum ± tennantite/tetrahedrite ($Cu[As,Sb]_4S_{13}$) ± chalcopyrite ($CuFeS_2$) (Appendix 2; Fig. 3-19).

Fig. 3-16 Relic bladed carbonate veins now pseudomorphed by quartz. Bladed carbonate veins are overprinted by adularia and siliceous alteration, which implies that they developed pre or synchronous with the onset of phyllic alteration (Table 3-3). Quartz flooding that pseudomorphs bladed carbonate occurs paragenetically later. '**A**': quarter core at Eunsan; quartz flooding hosts significant Ag mineralisation from acanthite in darker silica (EN042 23m, 2.82ppm Au, 696.80ppm Ag; scale bar shows cm intervals). '**B**': Chunsan; quartz pseudomorphing bladed carbonate (CH006 34.6m, 0.33ppm Au, 1.80ppm Ag; scale bar = 1cm).

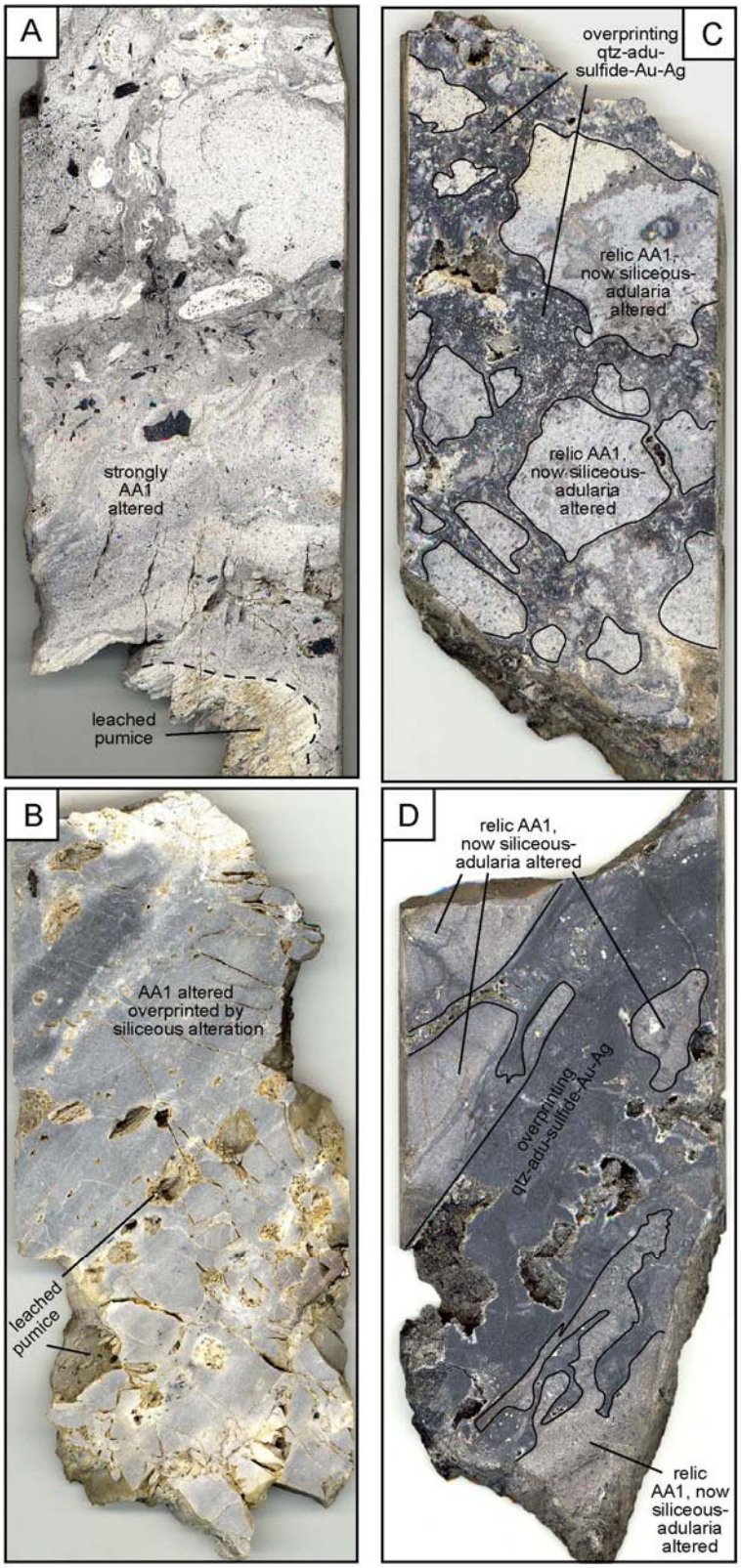

Fig. 3-17 Adularia-Au-Ag mineralisation at Chunsan cross cutting earlier advanced argillic alteration. '**A**' and '**B**' show advanced argillic 1 alteration (kaolinite-quartz alteration±leaching). 'B' now overprinted by siliceous alteration. '**C**' and '**D**' show relic patches of advanced argillic altered and leached rock overprinted by quartz-adularia-Au-Ag mineralisation (Figs. 3-18 & 3-19) and associated siliceous-adularia alteration. 'A' - CH006 180.5m (1m @ 0.08ppm Au & 5.6ppm Ag); 'B' - CH003 61.5m (1m @ 0.27ppm Au & 10.0ppm Ag); 'C' - CH003 135.5m (1m @ 1.93ppm Au & 88.4ppm Ag); 'D' CH003 146.5m (1m @ 1.14ppm Au & 54.8ppm Ag). Diamond drill core all ca. 5cm across.

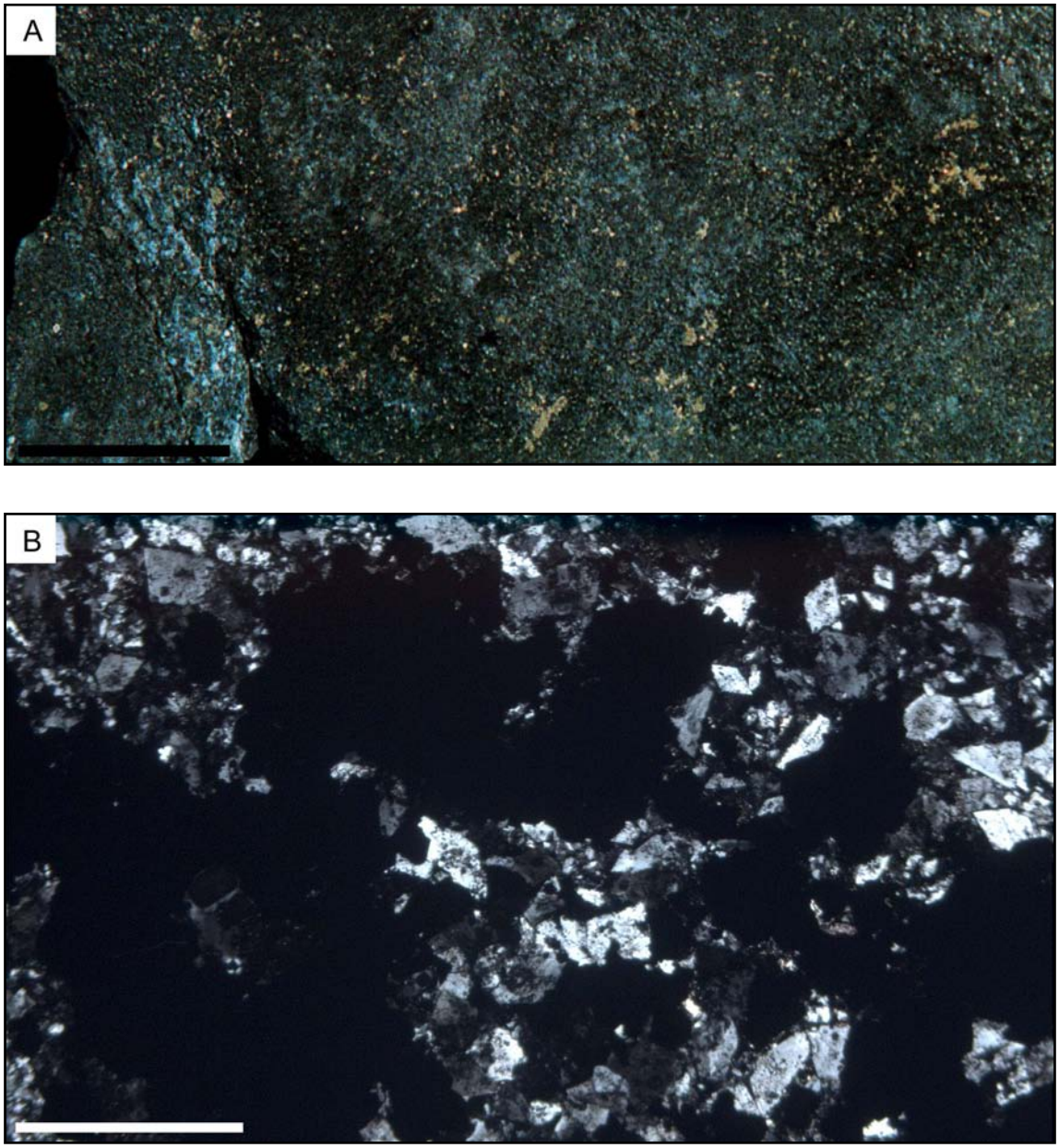

Fig. 3-18 Quartz-adularia-sulfide-Au-Ag mineralisation at Chunsan. Age data in Chapter 4 shows that disseminated adularia-Au-Ag mineralisation formed before vein adularia-Au-Ag mineralisation (Table 3-3). '**A**': drill core showing massive disseminated adularia-sulfide (CH003 115m, 24.02ppm Au, 70.2ppm Ag; scale bar = 2cm); '**B**': thin section shows massive abundant rhombic adularia crystals in siliceous-altered rock with pyrite (opaque material) (XPL, CH003 115m, 24.02ppm Au, 70.2ppm Ag; scale bar = 1mm).

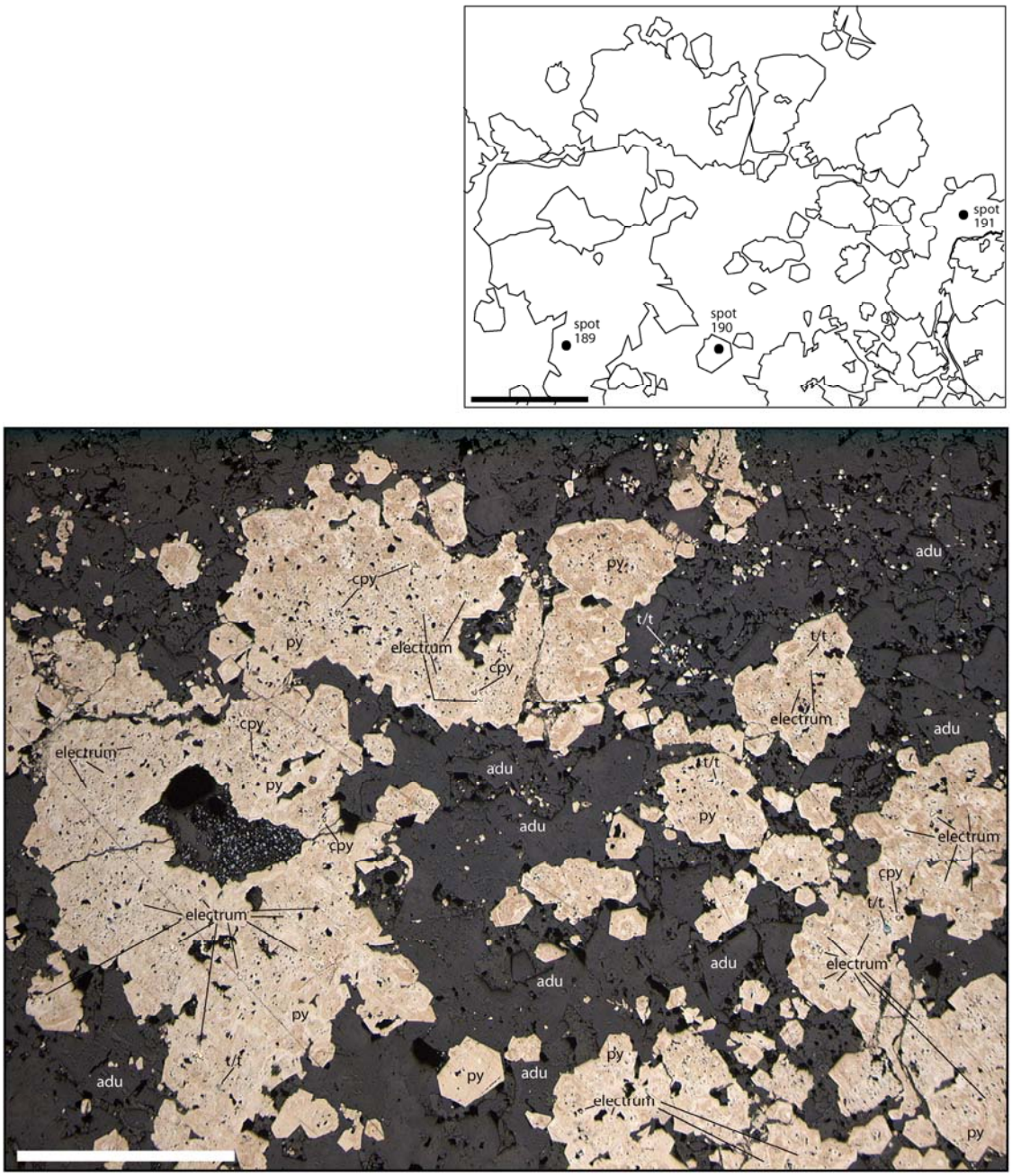

Fig. 3-19 Quartz-adularia-sulfide-Au-Ag mineralisation at Chunsan. Main photo showing abundant adularia-sulfide-Au-Ag mineralisation in thin section (RL, CH003 115m, 24.02ppm Au, 70.2ppm Ag; scale bar = 1mm). Note the euhedral rhombic adularia crystals. adu = adularia; py = pyrite; t/t = tennantite/tetrahedrite; cpy = chalcopyrite. Upper line diagram outline showing microprobe spot analyses (see Appendix 2 for microprobe data). Adularia alteration is directly associated with sulfide-Au-Ag mineralisation at Chunsan.

Siliceous alteration and quartz±adularia±Au-Ag-vein development at Eunsan and Moisan

Siliceous alteration is developed in core zones at Eunsan, Moisan and Chunsan, characterised by texturally destructive replacement by quartz (Table 3-3). Siliceous alteration forms zones between a few mm less than a metre wide, but can extend up to several metres locally.

Quartz-only veins are generally restricted to shallow levels, comprise crystalline quartz, are typically less than 2mm wide and have minimal siliceous-altered selvages. At Eunsan and Moisan, these veins are relatively common at surface (Fig. 3-20). At Chunsan, this style of veining is weakly developed as minor hairline quartz-only veinlets.

Quartz-only veining was followed by quartz±adularia±sulfide±Au-Ag veining (Table 3-3). These veins are predominantly restricted to core siliceous zones. This adularia vein event is paragenetically related to adularia alteration discussed previously (see page 3-32), however this adularia vein event is restricted to core zones whereas the adularia alteration occurs peripheral to siliceous-altered zones. This type of veining has not developed at Chunsan, instead, adularia and associated Au-Ag mineralisation at Chunsan is disseminated within muddy units and units that have undergone leaching (see page 3-32). However, the similar mineralogy of vein mineralisation at Eunsan and Moisan and disseminated mineralisation at Chunsan implies they are part of the same district-wide paragenetic event. Radiometric age data from the three systems (Chapter 4) confirms that the adularia-Au-Ag event at Chunsan overlaps with the adularia vein development at Eunsan and Moisan (Table 3-3).

At Eunsan, veins developed during this stage are associated with brecciation of earlier quartz-only and bladed carbonate veins. These vein-breccias grade inwards from slab breccia at their margins to fluidised sections with significant infill matrix hosting angular clasts of the adjacent wall-rock (Fig. 3-21A). Matrix infill is typically dominated by silica with a layer of mesocrystalline quartz less than 1mm thick rimming the clasts and the remaining void space filled by clear to cloudy, grey, massive to colloform banded cryptocrystalline quartz generally containing minor sulfide and Au-Ag. This silica flooding is most likely responsible for pseudomorphing earlier bladed carbonate veins.

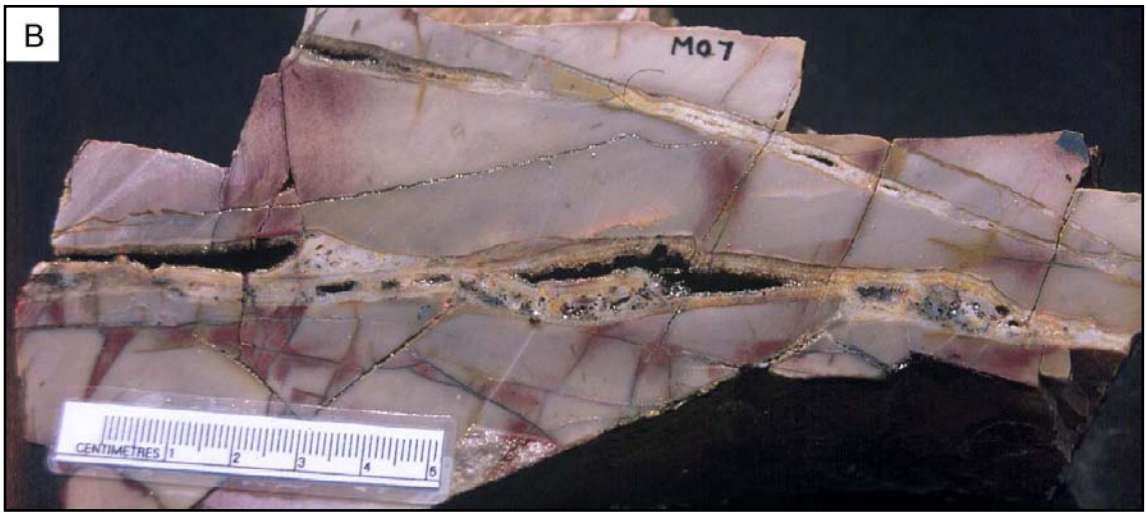

Fig. 3-20 Crystalline quartz-only veins. '**A**': sub-parallel steeply south dipping quartz-only stringer veins with siliceous altered selvages that make the rock resistant to weathering (sample location Moisan ●*087*, 0.30ppm Au, 0.8ppm Ag). '**B**': slab of 'A' highlighting the void space which is common to these quartz-only veins. Similar veins also occur at Eunsan but rarely at Chunsan.

At Eunsan, a second quartz±adularia-vein breccia event followed that previously described. This later stage of vein development is characterised by further brecciation of the previous silica dominated vein-breccia. The presence of mesocrystalline rimmed clasts characteristic of the initial vein-breccia within the second quartz vein-breccia event is clear evidence of two separate breccia events (Fig. 3-21B). The second vein-breccia event is generally dominated by sulfide but also contains zones of quartz-rich infill. Sulfide-dominant zones of infill typically include quartz ± adularia ± pyrite (FeS_2) ± Ag-sulfides (acanthite/argentite Ag_2S) ± Ag-sulfo salts proustite/pyrargyrite ($Ag_3[As,Sb]S_3$) and pearcite/polybasite ($[Ag,Cu]_{16}Sb_2S_{11}$) ± native Ag ± electrum(Ag-rich) ± minor base metals as Fe-poor sphalerite ([Zn,Fe]S), galena (PbS), chalcopyrite ($CuFeS_2$), tennantite/tetrahedrite ($Cu[As,Sb]_4S_{13}$) ± late carbonate (Appendix 2; Fig. 3-22). This stage of veining is the most economically significant at Eunsan. Quartz infill textures include crystalline to mesocrystalline banded quartz, colloform banded quartz and massive silica. Adularia infill generally forms tablets ca. 1mm in size.

At Moisan, a similar late stage of veining is also present, which shows similar quartz and adularia infill textures, sulfide assemblages and breccia development (Fig. 3-23). However, at Moisan this stage of vein development contains some different sulfide minerals from those at Eunsan. Where dominated by quartz at Moisan, these veins generally comprise colloform banded cryptocrystalline quartz to crustiform banded crystalline-mesocrystalline quartz ± adularia, with minimal sulfide or metal infill (Fig. 3-23A). Generally the quartz-adularia colloform-crustiform banded veins host moderate to high Au-Ag grades (ca. 1 to 50ppm Au and 100 to 500ppm Ag). Where dominated by sulfide (Fig. 3-23B), infill is typically colloform to crustiform banded quartz ± adularia ± pyrite (FeS_2), ± Ag±Au-rich tellurides (hessite Ag_2Te, empresite AgTe, krennerite $Au,AgTe_4$), ± native Te, ± Ag-sulfides (acanthite/argentite Ag_2S), ± Fe-poor sphalerite, ± galena, ± chalcopyrite, ± the goldfieldite ($Cu_3[Te,Sb]S_4$) to tennantite/tetrahedrite ($Cu[As,Sb]_4S_{13}$) series with variable substitution of Ag±Au for Cu (Fig. 3-24; Appendix 2). These sulfide-rich zones host the highest primary Au-Ag grades at Moisan, especially the diffuse colloform banded black silica (493ppm Au, 1300ppm Ag). Where base metal-rich, veins typically occur as distinctive crystalline banded quartz veins at depth, with base metal mineralisation dominated by Fe-poor sphalerite ± galena ± chalcopyrite with lesser amounts of goldfieldite/tennantite/tetrahedrite (Fig. 3-25; Appendix 2). Banded quartz veins at depth host the highest grade base metal mineralisation, containing up to ca. 1.8% Pb and Zn, and 0.3% Cu.

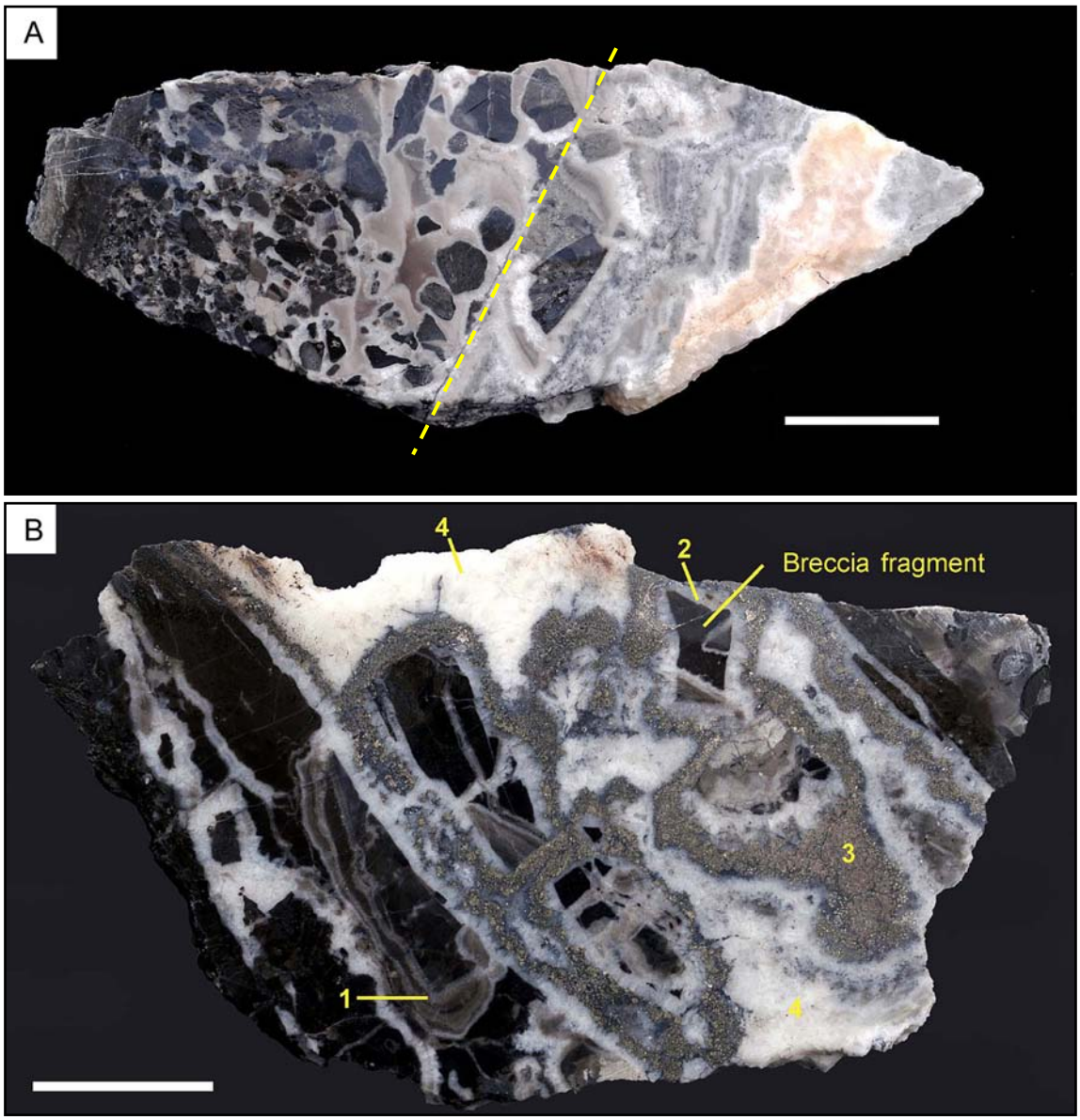

Fig. 3-21 Eunsan first and second vein breccia event. '**A**': the first vein-breccia event (left side) is overprinted by quartz dominant infill associated with the second vein-breccia event (right side). The first vein-breccia event is characterised by the distinctive silica rimmed clasts (left side) set within colloform banded to massive chalcedonic infill. Subsequently, re-brecciation during the second vein-breccia event has incorporated broken fragments of this first vein-breccia (evident as incomplete rimmed clasts) within the second vein-breccia matrix of mesocrystalline to crustiform-colloform banded quartz infill with acanthite, pyrite, and late-stage carbonate (far right side). '**B**': sulfide dominant second vein-breccia event (centre) overprinting first stage vein-breccia event (left and far right side). **1** – colloform banded silica infill from first vein-breccia event (equivalent to left side in 'A'). **2** – clast within second vein-breccia event showing characteristic first vein-breccia event silica rim. **3** – pyrite-acanthite-native Ag infill. **4** – overprinting late-stage carbonate infill. Photos courtesy Nicholson (2003), both scale bars = 3cm.

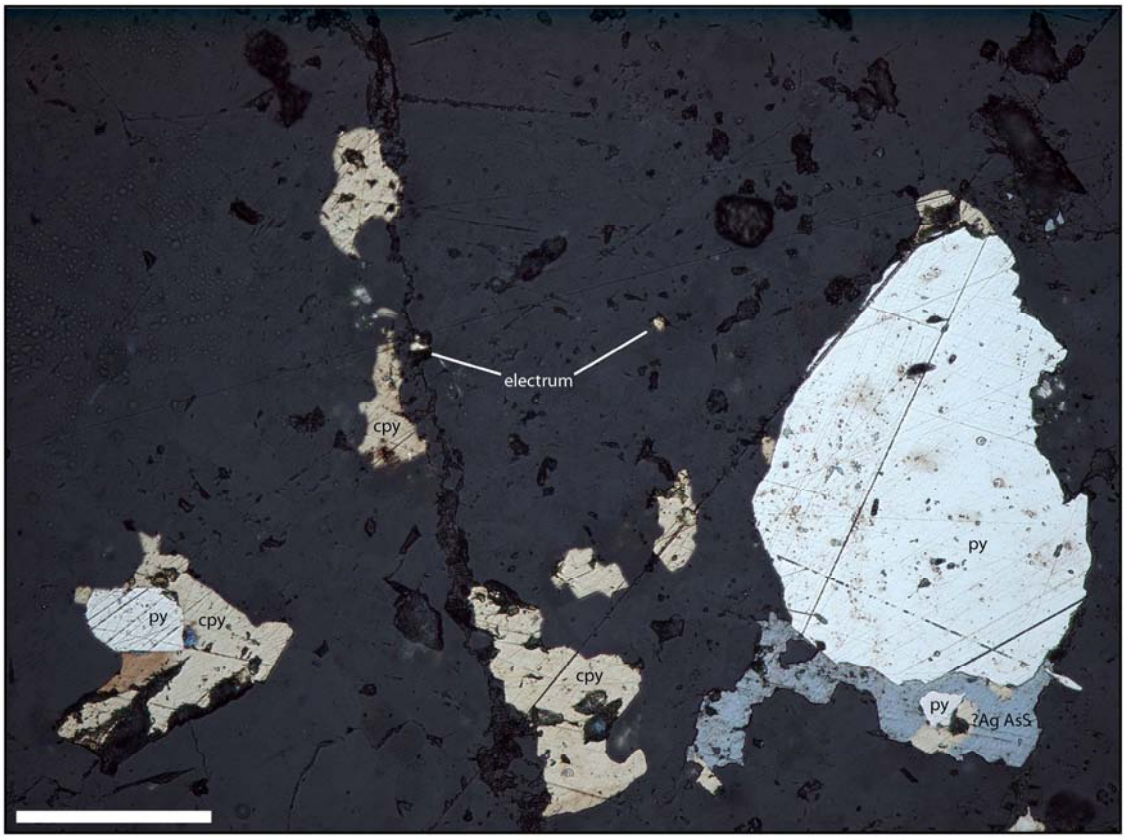

Fig. 3-22 Eunsan second vein breccia material with quartz-adularia-sulfide matrix infill. Main photo shows the sulfide mineralisation in thin section. This sample is unusually anomalous in visible chalcopyrite (cpy) compared to the majority of Eunsan mineralisation. Ag mineralisation is manifested as trace electrum grains hosted within quartz-adularia matrix. The grey mineral in the lower right corner is most likely proustite (Ag_3AsS_3); electron microprobe data returned 22.85wt% for S and 6.73wt% for As; total wt% 29.58 (RL, EN006 72m 1.66ppm Au, 230.60ppm Ag; no assay data for base metals; scale bar = 0.1mm). Upper line diagram outline shows the position of microprobe spot analyses (see Appendix 2 for microprobe data).

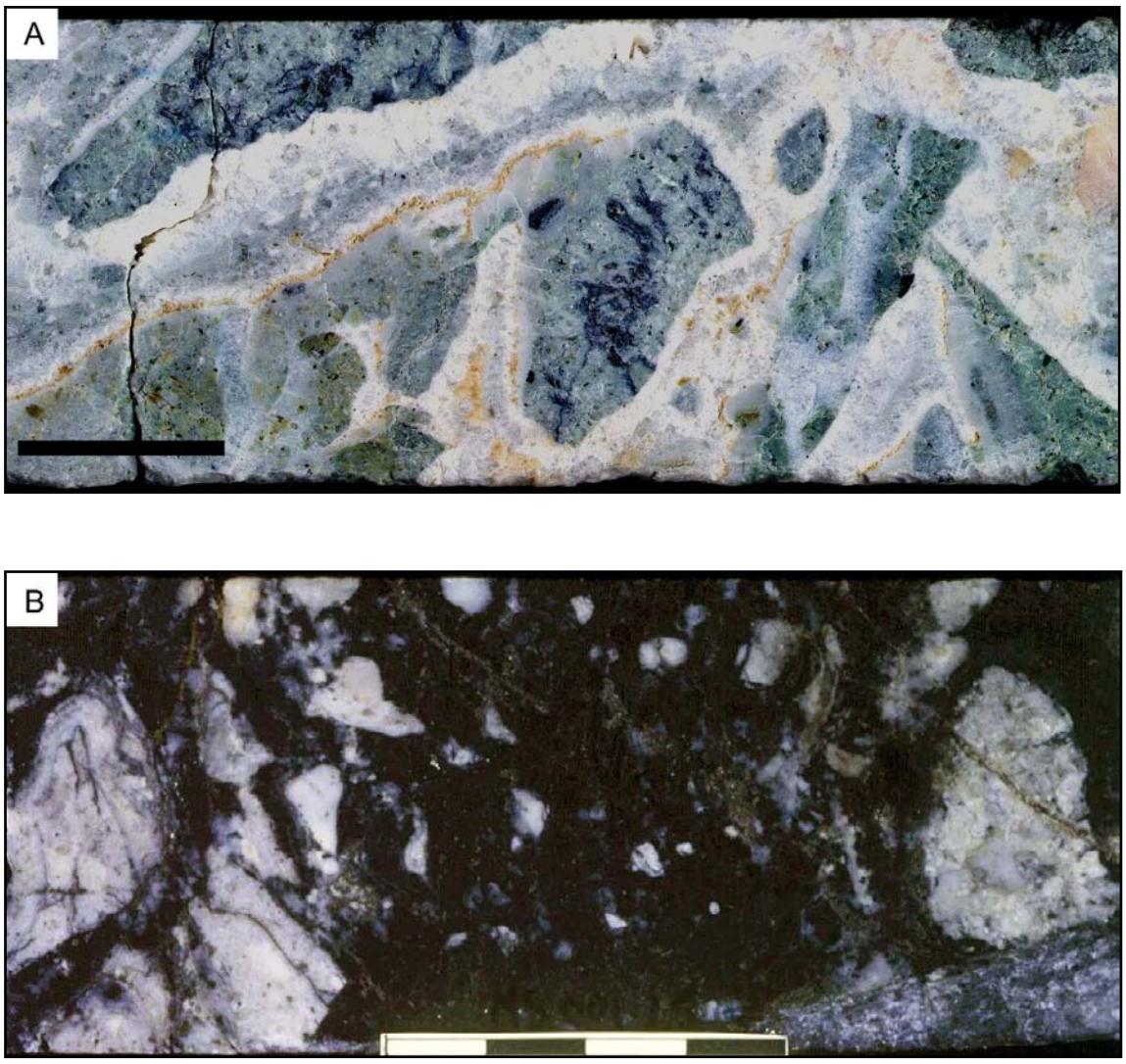

Fig. 3-23 Moisan quartz±sulfide mineralisation paragenetically equivalent to the second vein-breccia event at Eunsan. '**A**': crustiform crystalline to mesocrystalline quartz+adularia infill with some Ag-rich sulfide formed during the second vein-breccia event (MS008 147.8m 0.77ppm Au, 78.8ppm Ag; scale bar = 2cm). Adularia is distinctive as buff coloured vein material. '**B**': sulfide dominant veining comprising black silica-sulfide rich breccia with colloform sulfide-quartz infill material (MS001 110m 493.00ppm Au, 1300.0ppm Ag; scale bar cm graduations).

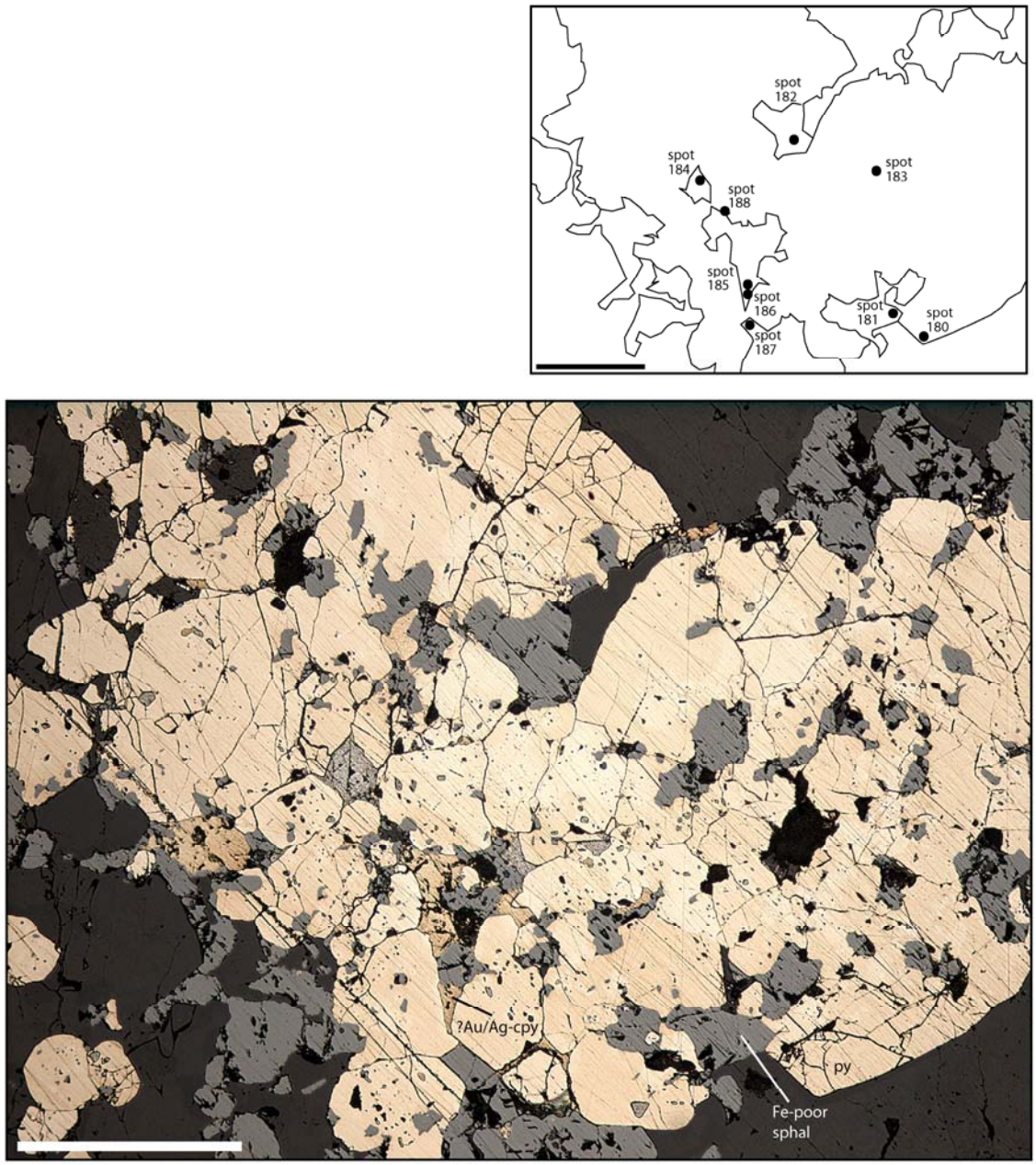

Fig. 3-24 Moisan quartz±sulfide vein material paragenetically equivalent to the second breccia event at Eunsan. Main photo shows the sulfide mineralisation in thin section. This sample contains significant pyrite (yellow) and Fe-poor sphalerite (grey) set in a quartz matrix. Fe-poor sphalerite wt% totals range from 60.72% to 96.48% and some chalcopyrite wt% totals are less than 60.72% possibly indicating Ag substitution (RL, MS007 76m 1.60ppm Au, 73.40ppm Ag; no assay data for base metals; scale bar = 0.25mm). Upper line diagram outline shows the position of microprobe spot analyses (see Appendix 2 for microprobe data).

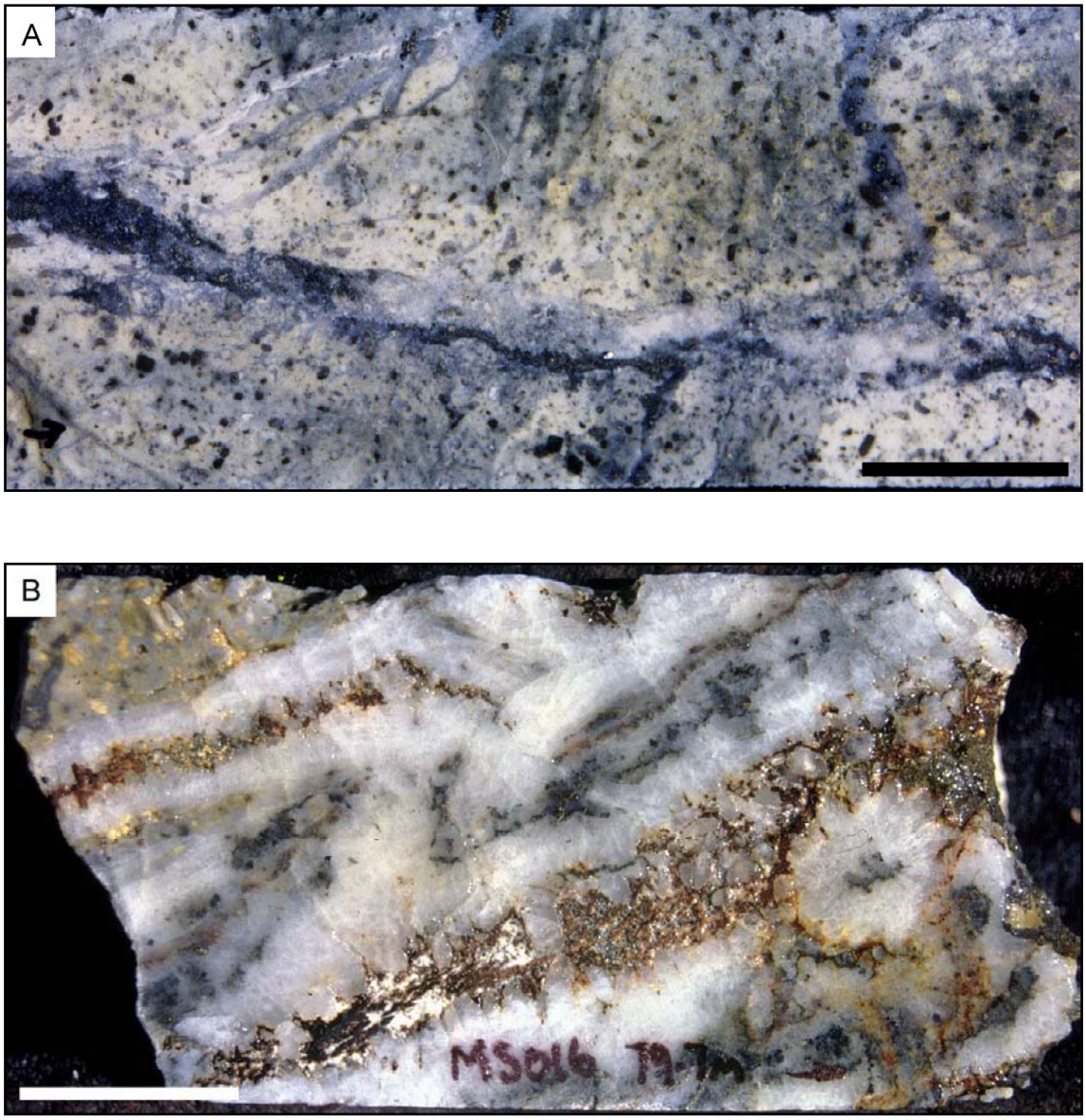

Fig. 3-25 Moisan base-metal mineralisation. '**A**': diffuse quartz-base-metal-sulfide veining (Fe-poor sphalerite+galena±minor chalcopyrite) (MS021 90.25m 0.94ppm Au, 34.4ppm Ag, 216ppm Cu, 2093ppm Pb, 4802ppm Zn; scale bar = 2cm). '**B**': coarse crystalline banded quartz-base-metal-sulfide±late stage carbonate veins (MS016 79.7m 5.15ppm Au, 39.8ppm Ag, 899ppm Cu, 313ppm Pb, 258ppm Zn; scale bar = 2cm).

Late-stage carbonate alteration and vein development

Late-stage massive carbonate-only veins and associated carbonate alteration overprint the phyllic-adularia-siliceous alteration and vein assemblages, and associated Au-Ag±base-metal mineralisation (Table 3-3). This late-stage carbonate event differs from the carbonate alteration developed within the propylitic and phyllic alteration stages. Late carbonate is distinguished primarily by its discordant cross cutting and overprinting relationship to adularia, phyllic and propylitic alteration. Late-stage carbonate-only veins and textures have been previously discussed within Sections 3.2 and 3.3. These overprinting late-stage carbonate-only veins and associated alteration occur within Eunsan, to a lesser degree at Moisan, and rarely at Chunsan.

Late-stage advanced argillic alteration ± supergene enrichment and/or depletion

Advanced argillic alteration has developed at Moisan (Table 3-3; Fig. 3-29) and is recognised by silica±kaolinite±hematite assemblage with rare alunite occurring locally as late infill. Remnants of the siliceous and phyllic alteration have been preserved within the advanced argillic alteration within a zone that extends from surface to approximately the base of oxidation. Below this boundary pyrite is ubiquitous, above this boundary, pyrite is absent.

Arribas Jr. (1995) summarises three distinct geological processes for the formation of an advanced argillic cap. These are: 1. magmatic-hydrothermal processes by disproportionation of magmatic SO_2 to H_2SO_4 and H_2S following adsorption by groundwater; 2. steam-heated processes by atmospheric oxidation of H_2S in the vadose zone over the water table, associated with fumarolic discharge of vapour released by deeper boiling fluids; or 3. supergene processes by atmospheric oxidation of sulfides during weathering.

The sub-horizontal boundary between the shallow near-surface advanced argillic cap and underlying phyllic alteration zones (Fig. 3-29) is clearly marked by high Pb and Zn values within the phyllic altered rocks and reduced (but still significantly anomalous) values of Pb and extremely low Zn values in the advanced argillic altered rocks. This may reflect the mobility of Zn within the weathering environment and the ability of Pb to form insoluble secondary Pb minerals (e.g. plumbojarosite). As a result Zn is removed and Pb is only slightly reduced. Cu is low in the advanced argillic zone and is often highly concentrated at the boundary with higher values (but still low) in the phyllic altered zones. The Cu concentration at the boundary is inferred to represent supergene enrichment at the water table. Ag values are consistently higher within this upper advanced argillic zone and a relatively sharp cut-off is often evident at the boundary. Ag values within crystalline quartz veins at surface host supergene enriched Au-Ag grades, up to ca. 100ppm Au, ca. 10,000ppm Ag (ca. 1% Ag). Additionally, the ubiquitous pyrite below this boundary and the absence of pyrite above it further highlight this transition

zone. The spatial coincidence of the advanced argillic alteration cap and geochemical enrichment and/or depletion of various metals at Moisan suggest both are primarily the result of supergene processes.

Steam-heated processes also appear to have had an active role in the generation of the advanced argillic alteration cap at Moisan. Arribas Jr. (1995) states that alunites forming in a steam-heated environment form with kaolinite and interlayered illite-smectites at about 100 to 160^{o}C where fumarolic vapour condenses above the boiling zone and form neutral pH, H_2S-rich fluid, typical of geothermal systems that form low-sulfidation deposits. Leach (2000) has documented widespread illite alteration and rare interlayered illite/smectite as well as localised cyclical alunite/illite alteration occurring at Moisan, implying that their development was characterised by steam-heated processes. Evidence for the boiling of hydrothermal fluids required to generate a steam-heated environment is observed at Moisan in the banded textures of the chalcedonic veins and the presence of adularia (Dong et al., 1995; Dong & Morrison, 1995). However, many of these veins occur within the upper advanced argillic zone, therefore the genesis of the advanced argillic cap could not be linked to boiling within these veins. The crystalline veins with coarse base-metal sulfides that appear later than the chalcedonic veins are generally recognised as deeper level veins that occur below the boiling zone (Dong et al., 1995). Therefore there has been some degree of fluctuation in the boiling level at Moisan. A number of the veins in the advanced argillic alteration have narrow alteration selvages that appear to overprint the advanced argillic alteration. These observations do not rule out the advanced argillic alteration as a result of boiling, (which could still be due to a deeper boiling system) but it does rule out a connection with observed adularia-Au-Ag veins.

Arribas Jr. (1995) states that magmatic-hydrothermal alteration would typically include alteration minerals such as diaspore, pyrophyllite, kaolinite, dickite and zunyite. Although alunite and kaolinite are present in the advanced argillic cap at Moisan, the fine grain-size and late infilling habit of these minerals and in light of the evidence for supergene and steam-heated processes as the dominant process in the genesis of the advanced argillic cap at Moisan, the possibility of magmatic-hydrothermal processes as a dominant process is unlikely.

Eunsan also shows evidence for geochemical enrichment and/or depletion by supergene processes, although no overprinting advanced argillic altered cap has been observed. The lack of an overprinting advanced argillic altered cap at Eunsan most likely reflects a lesser amount of sulfides compared with Moisan. Without primary sulfides, subsequent oxidation within the vadose zone would not produce sufficient surficial acidic waters to promote supergene enrichment, depletion and acid alteration.

Eunsan does however show zones of bonanza-grade Ag±Au mineralisation generally coincident with the base of oxidation. Within this zone, the average grade of 25 underground rock grab samples is 833.4ppm Au and 70,976ppm (7.1%) Ag, with a Ag:Au ratio of 85:1 (Nicholson, 2003). Samples from this zone are inferred to contain Ag remobilised by supergene processes. Where structures have permitted, this supergene enrichment zone has locally extended up to several metres below the general base of oxidation. Au does not show similar enrichment to Ag, reflecting the greater mobility of Ag within the weathering environment. However, Au does show localised surface enrichment. These bonanza Ag zones were only recognised during underground development. As such, limited information has been gathered for this project on these zones.

Eunsan also shows significant development of mineralised manganese infill within vein cavities above the base of oxidation. These manganese zones are inferred to have developed in response to supergene processes. They have been primarily recognised in underground development exposures, and comprise highly friable black manganiferous material that contains Au and Ag. These zones were rarely recovered by diamond drilling, with the manganiferous material most likely lost through circulating drilling water. As a result, limited information is available on this material.

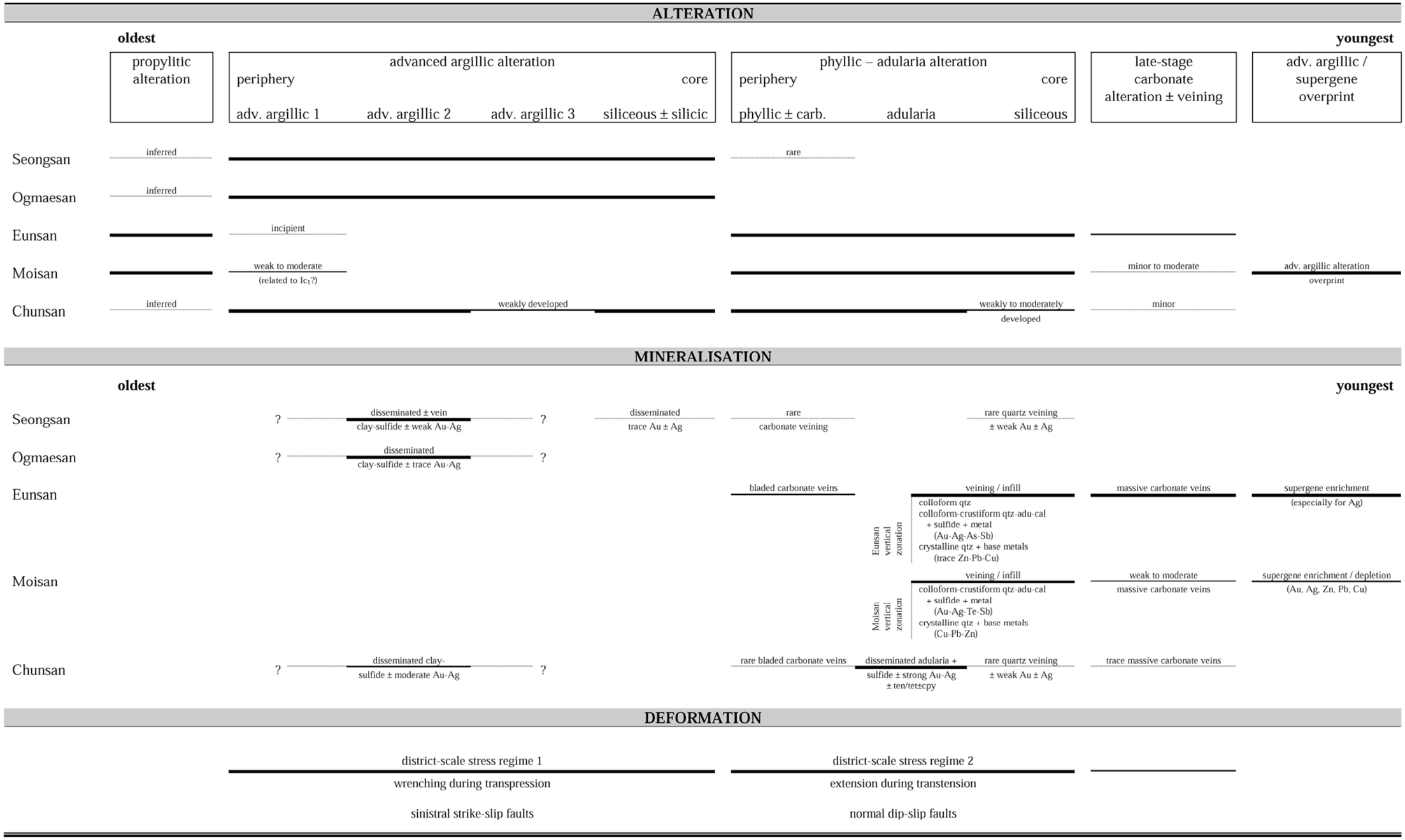

Table 3-3 Paragenetic events for all epithermal systems in the Seongsan district. Key relationships highlighted are that advanced argillic alteration dominates in some systems, whereas phyllic-adularia alteration dominates in others; however, Chunsan, and to a lesser degree, Seongsan epithermal systems comprise significant amounts of both alteration types. In addition, field relationships show that advanced argillic alteration pre-dates phyllic-adularia alteration across the district. Furthermore, field relationships also show that advanced argillic alteration and associated mineralisation formed on and around structures that were active during district-scale stress regime 1, whereas phyllic-adularia alteration and associated mineralisation formed on and around structures that were active during district-scale stress regime 2. Line thickness relates to abundance/intensity, with a thicker line indicating greater abundance/intensity. See Section 3.5 for further discussion between timing of structural and alteration/mineralisation events.

3.5 GEOLOGICAL SETTING OF EPITHERMAL DEPOSITS AND PROSPECTS WITHIN THE SEONGSAN DISTRICT

3.5.1 Geological setting of the Seongsan epithermal deposit

The Seongsan system is located on the southern peninsula in a valley at sea-level (Figs. 1-8, 1-9, 2-2; Appendix 6). The Seongsan system hosts a currently producing clay-sulfate mine, with four large operating open pits and one underground operation, plus numerous decommissioned old workings within an approximately 5km^2 area (Appendix 6). Underground mine workings as of September 2001 extend to ca. minus 100mRL. Open pits vary from small (<10m total cuts) to moderate size (multiple >10m benches).

Outcropping rock at Seongsan has undergone extensive advanced argillic alteration (excluding the volcaniclastic debris flow breccia unit AVdb and discordant rhyodacitic igneous complexes Ic_3). Mineralisation at surface is characterised by commercial grade kaolinite±dickite±alunite, and sub-economic disseminated precious metal mineralisation associated with the development of advanced argillic alteration (Section 3.2.3). Initial surface sampling within the Seongsan system by Ivanhoe Mines Ltd. returned peak assays of 5.82ppm Au and 12ppm Ag (Sangbong pit, Kirwin & Spadafora, 1994; Fig 2-23). Subsequent open pit sampling of the Bukok pit (Panther et al., 2000; Fig 2-23) returned peak assays of 0.48ppm Au and 26.4ppm Ag (n=97). Re-sampling of selected Seongsan Clay Mining Co. diamond drill core by Ivanhoe Mines Ltd. geologists confirmed an interval of 20m at 1.42ppm Au, 4.51ppm Ag with peak assay of 2.17ppm Au and 17.5ppm Ag corresponding to a 2m sample interval (DDH 88-6). These results highlight the relatively low-grade nature of Seongsan with respect to precious metal mineralisation, but that the advanced argillic zones are commercially exploitable clay and alunite resources.

3.5.1.1 Host rocks and field relationships at the Seongsan epithermal system

The Seongsan epithermal system is hosted by the Cretaceous Hwangsan Volcaniclastics unit (HV), the Hwangsan Tuff ignimbrite unit (HVf) and subvolcanic Ic_2 intrusions and extrusions (Fig. 3-26).

The volcaniclastic debris flow breccia unit AVdb is extensively exposed around the periphery of the Seongsan area, but is unaffected by advanced argillic alteration (Fig. 3-26). Alteration and mineralisation at Seongsan are confined to rocks that pre-date the deposition of AVdb. Ic_3 intrusions south of Seongsan show no evidence of advanced argillic alteration. Ic_1 has not been recognised occurring within the Seongsan area.

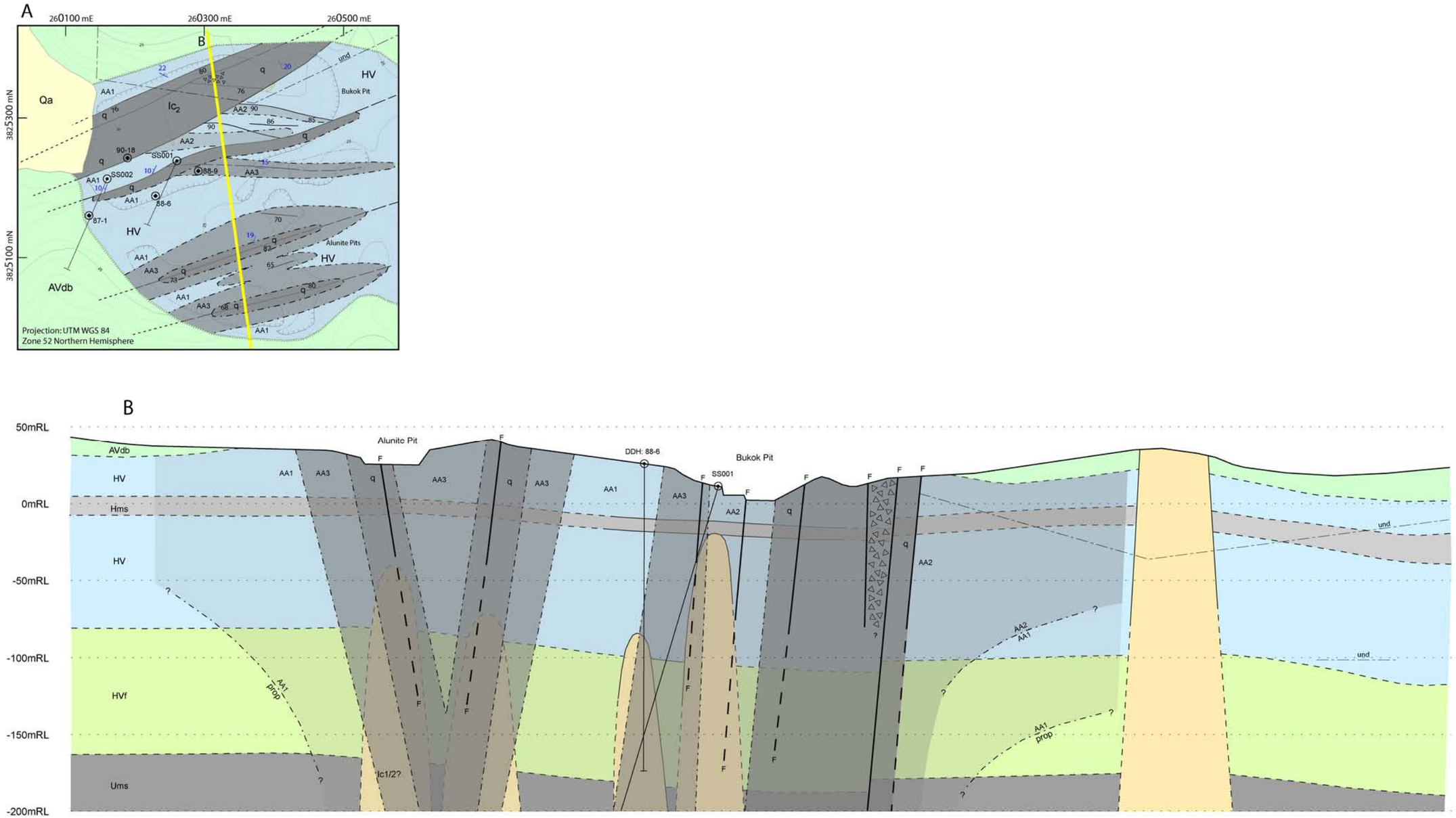

Fig. 3-26 Seongsan alteration zonation superimposed over geology and structure. Key relationships highlighted are that the advanced argillic alteration is formed around the principal faults of the Seongsan Fault Zone, and as a result, form tabular, steeply dipping east-northeast and east-southeast striking zones. '**A**': plan view of the Seongsan system, focused around the Bukok and Alunite open pits showing lithology, structure and alteration zonation, and diamond drill hole collar locations and traces for Ivanhoe Mines Ltd. (SS001 and SS002) and Seongsan Mining Co. (vertical holes 88-9, 88-6, 87-1 and 90-18) (see Fig. 2-2 for map bounds location). '**B**': cross section view as outlined in 'A' (looking west) showing lithology, structure and alteration as determined from surface mapping and some diamond drill hole data. Due to a lack of available diamond drill hole data for this area and very limited underground access, alteration zonation and lithologies have primarily been projected from surface, hence they may appear simplified but they cannot be resolved any further based on current data. Propylitic alteration boundaries have been inferred and may actually occur well outside the Seongsan system. Note: the view in 'B' shows an extended cross section compared to that outlined in 'A'. DDH: 88-6 (Seongsan Mining Co.) is ca. 100m off section to the west and SS001 is ca. 80m off section to the west. Alteration assemblages comprise the following: prop = propylitic; AA1, AA2, AA3 = advanced argillic 1, 2, 3 (see Table 3-1); and q = siliceous. Relic patchy phyllic and carbonate alteration observed at Seongsan overprinting advanced argillic alteration (as documented in Section 3.4.2.1) occur within SS001 at 298m. Dashed lines inferred; annotations 'F' label faults and 'und' label underground mining operations in section; lithology labels as per Section 2.2. See main text for further detail.

3.5.1.2 Structural setting of the Seongsan epithermal system

The Seongsan system is located within the Seongsan Fault Zone (Figs. 2-23, 3-26). The sinistral and then normal sense and direction of offset on this fault zone are well constrained from detailed mapping (see: Chapter 2, Section 2.3.3.1; Figs. 2-24, 2-25, 2-27, 2-36). The bounding faults of the Seongsan fault zone strike east-northeast and dip steeply to the south, while shorter linking faults strike east-southeast and dip between steeply to the south and sub-vertical.

In addition to faulting, several breccia bodies have also developed within the Seongsan Fault Zone (Section 2.3.3.1; Fig. 2-24A). Breccias are localised at some of the junctions between the more extensive east-northeast-striking bounding faults and the shorter east-southeast-striking linking faults. The breccias at Seongsan are subvertical pipe-like bodies' ca. 10 to 20m in diameter. Texturally the breccias show angular jigsaw-fit clasts derived from Hwangsan Volcaniclastic unit HV set in a rock flour matrix. Both clasts and matrix show pervasive intense silicification. The most intense alteration in the Seongsan system occurs within these breccia zones and bounding faults (Fig. 3-26; Appendix 6). They are inferred to represent the main fluid ascent paths, i.e. core alteration zones. Adjacent alteration zones are inferred to represent outflow zones, peripheral alteration zones to the main fault-controlled conduits (Section 3.4.1). The localised occurrence of the silicified breccia bodies at the junctions of faults, their subvertical pipe-like nature and the locally derived angular jigsaw-fit clasts all suggest that the breccia bodies at Seongsan developed during sinistral strike-slip movement on the main Seongsan Fault Zone (Section 2.3.3.1; Fig. 2-24A). If formed during normal movement, a more gently plunging orientation might be expected.

The discordant nature of the main alteration zones with respect to bedding and offset of stratigraphic marker units across the steeply dipping planar zones of alteration supports this fault-controlled scenario. If bedding was the primary control on fluid flow, gently dipping core zones of silicification would be expected. Additional oxygen isotope data presented within Chapter 5 is also consistent with a vertical ascent for the hydrothermal fluids.

While intense siliceous alteration is developed along the larger east-northeast striking faults, the shorter east-southeast striking linking faults tend to be characterised by advanced argillic assemblages (Table 3-3). Sub-horizontal slickenlines developed on these shorter linking fault surfaces suggest that advanced argillic alteration took place before or during strike-slip movement (Section 2.3.3.1). These shorter linking faults typically show abundant clay and/or sulfate developed on their surfaces. In some areas, clay and/or sulfate are developed over several metres away from these faults. Zones of clay-sulfate mineralisation associated with

advanced argillic alteration exploited for dickite and alunite are focused on the margins of the main Seongsan Fault Zone and along shorter linking faults.

Porous stratigraphic units have had some control on advanced argillic alteration zonation away from the faults. Subtly stronger advanced argillic alteration extends for distances of 10s of metres along particular HV beds away from the main fault-controlled conduits.

After sinistral strike-slip movement and advanced argillic alteration, normal dip-slip movement occurred on the controlling faults (Section 2.3.3.1; Fig 2-25). This last phase of movement caused brittle fracturing of the siliceous alteration and development of steeply dipping slickenlines along the north-bounding faults of the Seongsan Fault Zone (Fig. 2-22). Fracturing of the siliceous altered rock shows that steeply south-dipping normal movement post-dates development of advanced argillic alteration.

Advanced argillic alteration at Seongsan appears to have developed during district-scale stress regime 1, which is characterised by wrenching during transpression (Section 2.3; Table 3-3). The normal faulting offsets the siliceous alteration whereas evidence in the surrounding district suggests that the later phyllic-carbonate alteration and veining at Seongsan formed during district-scale extensional stress regime 2, which is characterised by extension during transtension (Section 2.3; Table 3-3).

3.5.2 Geological setting of the Ogmaesan epithermal deposit

Ogmaesan is the most prominent hill in the district (167.9m) and is located near the north-western boundary of the Seongsan district (Figs. 1-8, 1-9, 2-2; Appendix 6). The Ogmaesan system has previously been exploited as a commercial source of kaolinite±dickite±alunite within an approximately 5km^2 area, but reserves have been depleted and mining has stopped.

Outcropping rock at Ogmaesan has undergone extensive advanced argillic alteration. Mineralisation at surface is characterised by patchy commercial grade kaolinite±dickite±alunite. From 45 surface rock grab samples (this study), the highest Au assay is 0.16ppm (<0.5ppm Ag), with remaining samples generally containing less than 0.10ppm Au. Highest Au grades at Ogmaesan are best developed within pyritic breccia matrix or advanced argillic altered units that contain disseminated pyrite (n=5: average 0.10ppm Au, 381ppm As; peak 0.16ppm Au, 676ppm As). No higher Au grades or vein-hosted Cu-Au-As sulfides that might be associated with higher Au grades have been detected within the Ogmaesan system to date. These results highlight the particularly weak nature of precious metal mineralisation at Ogmaesan.

3.5.2.1 Host rocks and field relationships at the Ogmaesan epithermal system

The Ogmaesan epithermal system is hosted by Cretaceous Hwangsan Volcaniclastics unit HV and discordant Cretaceous sub-volcanic intrusions and extrusions Ic_2 (Fig. 3-27). The volcaniclastic debris flow breccia unit AVdb is restricted to small coastal outcrops south of Ogmaesan (Fig. 2-2). At these locations, field relationships show that AVdb unconformably overlies the rocks that host Ogmaesan. Alteration and mineralisation at Ogmaesan are confined to the rocks that pre-date deposition of the volcaniclastic debris flow breccia unit AVdb. Ic_1 and Ic_3 have not been recognised within the Ogmaesan area. No drilling data is available from Ogmaesan and so examination was limited to surface exposures.

3.5.2.2 Structural setting of the Ogmaesan epithermal system

The Ogmaesan high-sulfidation hydrothermal system is primarily focussed on the main breccia body at Ogmaesan (Figs. 2-23, 3-27). Igneous complexes (Ic_2) appear to have locally focussed smaller zones of alteration development. The structural setting of the Ogmaesan main breccia and intrusives are well constrained from detailed mapping (Appendix 6).

The main breccia body at Ogmaesan is a subvertical pipe-like body ca. 200m in diameter that cuts through Hwangsan Volcaniclastic units HV (Fig. 3-27). Clasts generally comprise various rocks from within the Hwangsan Volcaniclastic unit HV. Clast are generally subrounded to subangular, well sorted and range in size from 1 to 8cm, typically 2 to 3cm, with rare metre-scale megaclasts. The matrix is predominantly rock flour. Both clasts and matrix have undergone pervasive intense silicification which can be texturally destructive. Silicification is accompanied by pink cryptocrystalline massive alunite infill. Moderate leaching to weak vuggy silica texture occurs within some clasts and/or the matrix locally. No sulfide mineralisation was observed within the breccia.

The pipe-like morphology of the breccia, its location at the centre of the zone of most intense alteration, the well sorted nature of the clasts, and their polymict subrounded character within a matrix dominated by rock flour, all suggest that this breccia represents the primary fluid ascent zone at Ogmaesan. Primary controls on the location of the main breccia at Ogmaesan have not been unequivocally resolved.

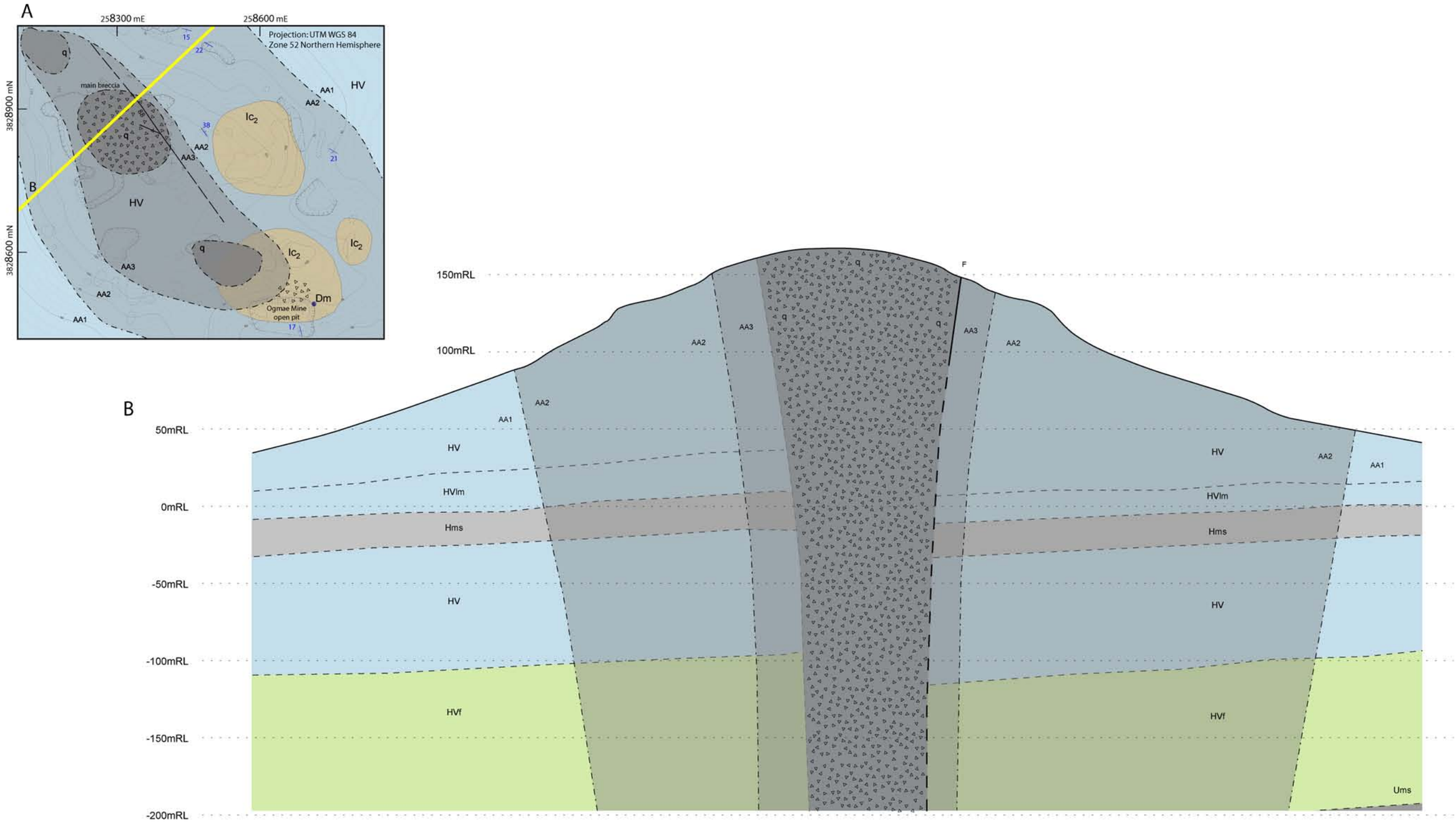

Fig. 3-27 Ogmaesan alteration zonation superimposed over geology and structure. '**A**': plan view of the Ogmaesan system, in the vicinity of the main breccia and Ogmae mine open pits showing lithology, structure and alteration zonation (see Fig. 2-2 for map bounds location). '**B**':- cross section view as outlined in 'A' (looking northwest) showing lithology, structure and alteration as determined from surface mapping. This cross section is at the same scale as the Seongsan cross section (Fig. 3-26). Due to the lack of diamond drill hole data in this area, alteration zonation and lithologies have been projected from surface, hence may appear simplified, but can not be resolved any further. Note: the view in 'B' shows an extended cross section compared to that outlined in 'A'. Alteration assemblages comprise the following: AA1, AA2, AA3 = advanced argillic 1, 2, 3 (see Table 3-1); and q = siliceous. Dashed lines inferred; annotation 'F' labels faults; lithology labels as per Section 2.2. See main text for further detail.

Other breccia bodies have developed within the Ogmaesan system. The breccia body within the Ogmae mine is also a subvertical pipe-like body, although only ca. <80m in diameter (Fig 3-27A). This breccia body within the Ogmae mine is exposed over 30m vertically. It is characterised by monomict buff coloured igneous complex Ic_2 jigsaw-fit angular to lesser subangular clasts that range between 0.5 to 10cm in size. The breccia is clast supported at margins to matrix supported away from margins. The matrix comprises smaller clasts and rock flour. Overall both matrix and clasts within this breccia have undergone pervasive advanced argillic 2 kaolinite±dickite alteration with strong brick red hematite alteration of the matrix. Clasts have not been affected by the hematite alteration. No silicification or sulfide mineralisation was observed at surface within the breccia. This breccia body is localised within igneous complex Ic_2. Textures suggest an intrusion-style breccia system, most likely developed in response to the emplacement of igneous complex unit Ic_2.

Apart from the main breccia body at the summit and the breccia body within the Ogmae mine, breccia development at Ogmaesan is limited to localised outcrop scale breccia occurrences generally <10m in extent. These small outcrop scale breccias show weak to moderate sulfide mineralisation generally disseminated within matrix and clasts.

Mapping of alteration zonation and overprinting relationships between alteration and bedding at Ogmaesan indicates that the most intense alteration is focused on the main breccia body at Ogmaesan. Peripheral alteration zones concentrically surround this core zone centred on the main breccia body. These relationships indicate that the main breccia body at Ogmaesan was the most likely primary fluid up-flow conduit at Ogmaesan. As hydrothermal fluids ascended through the main breccia body generating intense siliceous alteration, subsequent fluid out-flow through the surrounding rocks resulted in peripheral advanced argillic alteration assemblages (Section 3.4.1; Table 3-3). No significant focussing faults have been recognised at Ogmaesan. Fluid out-flow away from the main breccia body is not focussed in extensive steeply dipping planar zones like at Seongsan. As a result, ore-grade clay and sulfate occurrences are restricted to scattered patches ca. 10s to 100s of metres wide throughout the broader zone of advanced argillic alteration. Porous units have had some control on the extents of alteration, but this has been limited to localised areas up to 10s of metres wide and thick. Where fluid out-flow has intersected igneous complexes at Ogmaesan, rock competency contrasts and intrusive contact zones appear to have locally controlled fluid flow and subsequent alteration zonation around the igneous complexes. Units that have a relatively homogeneous composition (e.g. ash tuff) are generally pervasively replaced by massive kaolinite±dickite±pyrite(±alunite) whereas units that have a more heterogeneous composition (e.g. lithic/pumice tuffs) generally show selective replacement of the matrix by medium- to fine-grained kaolinite±dickite±pyrite(±alunite).

Age data (Chapter 4) shows that alteration at Ogmaesan and Seongsan was essentially synchronous. Advanced argillic alteration at Ogmaesan probably therefore also occurred during district-scale wrenching stress regime 1 (Section 3.2; Table 3-3). No evidence of an overprinting phyllic±adularia quartz veining event was seen at Ogmaesan like that at Seongsan, perhaps reflecting the apparent lack of potentially reactivated faults in this area.

3.5.3 Geological setting of the Eunsan epithermal deposit

Eunsan is situated on the coast where altered and mineralised rocks form a low-lying east-southeast striking ridge (Figs. 1-8, 1-9, 2-2; Appendix 6). The Eunsan system is a high-grade vein hosted Au-Ag deposit which began commercial production for Au and Ag in August 2002. The inferred resource at start-up was 251,800 tonnes, grading 15.0ppm Au and 83.8ppm Ag. No further publicly available resource data is currently available.

Siliceous alteration and associated mineralised veins form the core of the Eunsan deposit. Siliceous alteration is surrounded by either adularia or phyllic alteration assemblages. Mineralisation at surface is hosted by high-grade Au-Ag-bearing crystalline quartz veins ca. 1-10cm wide and vein breccias up to 1m wide. Initial surface sampling at Eunsan by Ivanhoe Mines Ltd. returned peak assays of 56.31ppm Au and 707ppm Ag (22.7oz).

3.5.3.1 Host rocks and field relationships at the Eunsan epithermal system

The Eunsan system is hosted by Hwangsan Volcaniclastics unit HV, the Hwangsan Tuff ignimbrite HVf and Uhangri Formation sediments Ums (Fig. 3-28). The volcaniclastic debris flow breccia unit AVdb is exposed in coastal outcrops ca. 100m south of the main Eunsan system. Generally, mineralisation is best developed within the upper Hwangsan Volcaniclastics unit HV, rather than the underlying Hwangsan Tuff unit HVf or the Uhangri Formation sediments Ums. No igneous complexes (Ic_1, Ic_2, or Ic_3) have been intersected in drilling at Eunsan. The closest igneous complexes are the conformable intrusive and extrusive dacitic to rhyolitic igneous complexes Ic_1 within the volcanic pile at Moisan ca. 1km to the north, and various occurrences of discordant intrusive dacitic to rhyolitic igneous complexes Ic_2 ca. 1-2 km to the east, south and southeast on the Seongsan peninsula.

3.5.3.2 Structural setting of the Eunsan epithermal system

The Eunsan system is focussed around the main fault at Eunsan, which strikes east-southeast and dips subvertical (Figs. 2-23, 3-28). Sinistral-reverse movement followed by normal movement are inferred on this fault (see: Chapter 2, Section 2.3.3.3; Figs. 2-29, 2-30, 2-31, 2-32, 2-36).

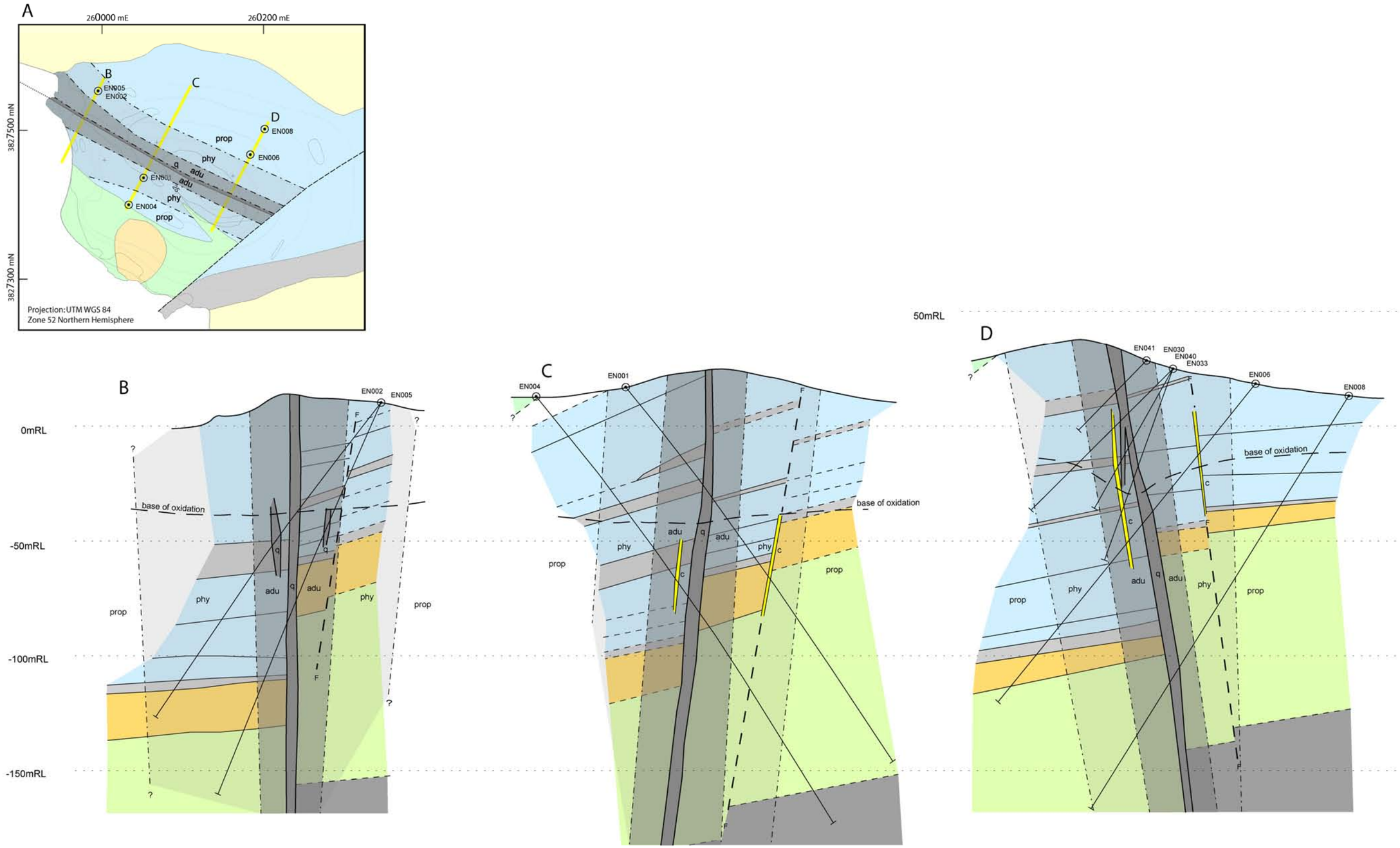

Fig. 3-28 Eunsan alteration zonation superimposed over geology and structure (from Fig. 2-29). Siliceous alteration, adjacent adularia alteration and related auriferous veining are localised around the main Eunsan Fault. Lithological unit labels have been removed (see Fig. 2-29 for labels). '**A**', '**B**', '**C**' and '**D**' views as per Figure 2-29. Alteration assemblages comprise the following: prop = propylitic; phy = phyllic; adu = adularia; q = siliceous; and c = carbonate (see Table 3-1). See main text for further detail.

Alteration zonation at Eunsan is focussed around the main vein and host fault. Alteration associated with mineralisation at Eunsan extends ca. 50m outwards from the main structure. The discordant nature of the vein and alteration zonation to bedding indicates that bedding in the host rocks was not a primary control on the distribution of alteration and mineralisation at Eunsan (Fig. 3-28).

Generally there is a main vein ca. 2 to 10m wide with sub-parallel minor veins ca. 1 to 2m that splay off either side (Section 2.3.3.3; Fig. 2-31). The steep dip and parallel strike of the splays imply they developed during the later phase of normal movement on the Eunsan Fault (Section 2.3.3.3; Fig. 2-31). These field relationships imply that phyllic-adularia alteration and associated mineralisation at Eunsan developed during district-scale extensional stress regime 2 (Section 2.3; Table 3-3).

3.5.4 Geological setting of the Moisan epithermal prospect

Moisan is ca. 1200m north of Eunsan, where altered and mineralised rocks form a prominent east-southeast-striking ridge (Figs. 1-8, 1-9, 2-2; Appendix 6). Moisan is currently an intermediate- to advanced-stage exploration prospect.

Mineralisation at Moisan is hosted by a series of discontinuous, thin 2 to 3cm wide, Au-Ag bearing quartz veins and ca. 5 to 10cm wide coarsely banded chalcedonic to crystalline quartz veins. Initial surface sampling at Moisan by Ivanhoe Mines Ltd. returned peak assays of 112.29ppm Au and 11,910ppm Ag (397oz).

3.5.4.1 Host rocks and field relationships at the Moisan epithermal system

The Moisan system is hosted by Hwangsan Volcaniclastics unit HV, heterolithic crystal-rich lapilli tuffaceous sediments HVxo and Hwangsan Tuff ignimbrite HVf (Fig. 3-29). Igneous complex Ic_1 is intersected in drill core at Moisan, forming a conformable part of the volcanic pile. Generally, alteration and mineralisation at Moisan are most extensive within the upper Hwangsan Volcaniclastics unit HV, and on the margins of Ic_1 and to a lesser extent within Ic_1, rather than the underlying lapilli tuffaceous sediments HVxo and Hwangsan Tuff unit HVf. Discordant intrusive dacitic to rhyolitic plugs (Ic_2) occur ca. 1km to the east-southeast and ca. 2 to 3km to the south and southwest. The closest exposure of the volcaniclastic debris flow breccia unit AVdb to Moisan is ca. 1km to the south at Eunsan.

3.5.4.2 Structural setting of the Moisan epithermal system

The Moisan system is located within the Moisan Fault Zone, a ca. 50m wide fault zone that strikes east-southeast and generally steeply dips to the south (Figs. 2-23, 3-29). An unresolved

component of sinistral followed by normal offset are inferred on this fault (see: Chapter 2, Section 2.3.3.3; Figs. 2-33, 2-34, 2-36).

The main faults within the Moisan Fault Zone appear to be the primary control on the location of alteration and mineralisation (Fig. 3-29). Mineralisation at Moisan is hosted by veins, vein breccias and shear zones. Mineralisation shows a strong spatial association with the margins of the dacite complex Ic_1. This may reflect a significant competency contrast between Ic_1 and the adjacent heterolithic lapilli tuffaceous sediments HVxo and Hwangsan Volcaniclastic unit HV. Within the upper HV units, vein development appears to have been more widespread compared to vein development in the HVxo unit (Fig. 3-29). Coherent zones of mineralisation like that observed at Eunsan are difficult to define. Higher grade mineralisation is not commonly observed in the units below the dacite complex Ic_1.

Age data (this study; Chapter 4) shows that mineralisation at Eunsan, Moisan and Chunsan was synchronous. Therefore, correlation with Eunsan suggests that mineralisation at Moisan would likely have developed during district-scale extensional stress regime 2 (Section 2.3; Table 3-3; Section 3.5.3).

Minor post-mineral faulting at Moisan has caused localised offset of the altered rocks. However, significant offset of veining has not been recognised.

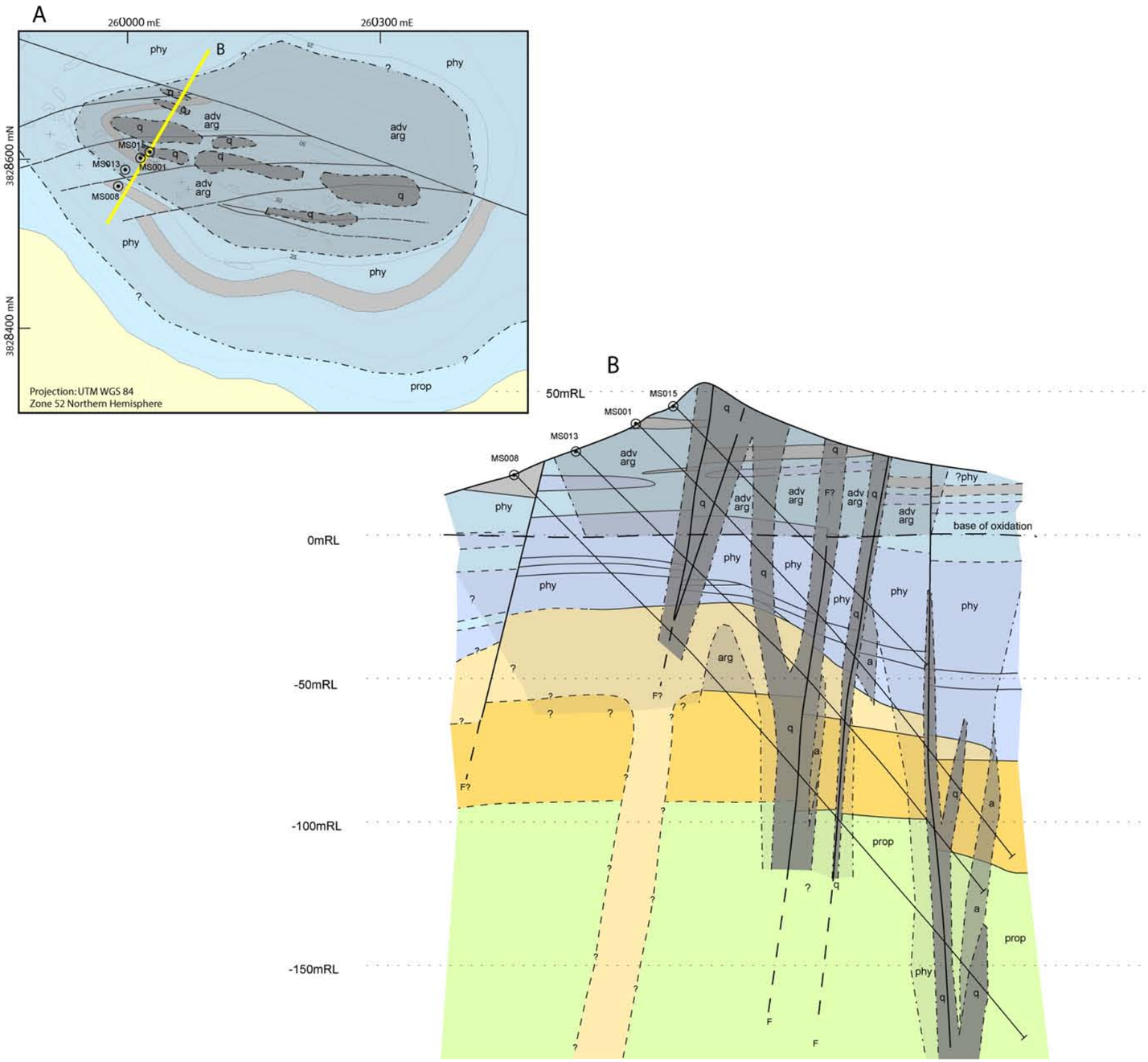

Fig. 3-29 Moisan alteration zonation superimposed over geology and structure (from Fig. 2-33). Siliceous alteration, adjacent adularia alteration and related auriferous veining are localised along the main faults that make up the Moisan Fault Zone. Lithological unit labels have been removed (see Fig. 2-33 for labels). '**A**' and '**B**' views as per Figure 2-33. Alteration assemblages comprise the following: prop = propylitic; phy = phyllic; adu = adularia; arg = advanced argillic 1; adv arg = advanced argillic 2/3; and q = siliceous (see Table 3-1). See main text for further detail.

3.5.5 Geological setting of the Chunsan epithermal prospect

Chunsan is located 2km northwest of the Bukok pit at Seongsan, and within 250m of several small-scale clay workings. Altered and mineralised rocks form a low-lying hill in which the ridge strikes broadly east-southeast (Figs. 1-8, 1-9, 2-2; Appendix 6).

Mineralisation at Chunsan surface is hosted by Au-Ag bearing silicified breccias and minor Au-Ag-bearing quartz veins. Quartz vein material at surface is characterised by saccharoidal to chalcedonic to mesocrystalline quartz, crudely colloform banded quartz and bladed quartz pseudomorphs after carbonate. These veins are not observed in diamond drill core from deeper in the system. Initial surface sampling at Chunsan by Ivanhoe Mines Ltd. returned peak assays of 8.58ppm Au and 10.2ppm Ag from 119 samples, of which 30% were over 0.1ppm Au.

3.5.5.1 Host rocks and field relationships at the Chunsan epithermal system

The Chunsan system is hosted by Hwangsan Volcaniclastics unit HV (Fig. 3-30). The volcanic debris flow breccia AVdb is exposed ca. 500m to the north of Chunsan. No igneous complexes (Ic_1, Ic_2, or Ic_3) have been observed at Chunsan. The closest igneous complexes are various occurrences of discordant intrusive dacite and rhyolite Ic_2 ca. 500m to the north and 1 to 2 km to the south.

3.5.5.2 Structural setting of the Chunsan epithermal system

The Chunsan system is located within the Chunsan Fault Zone, a ca. 50 to 80m wide fault zone that strikes east-southeast and dips steeply to the south (Figs. 2-23, 3-30). The sense and direction of offset on this fault zone have not been resolved. The Chunsan Fault Zone appears similar in character to the Moisan Fault Zone. This correlation implies sinistral followed by later normal offset (see: Chapter 2, Section 2.3.3.3; Fig. 2-35, 2-36).

Outcropping rock at Chunsan is dominated by breccia. The breccia resembles cataclasite material with jigsaw-fit clasts and limited matrix. Clasts comprise rocks from the Hwangsan Volcaniclastics (HV). Clasts are angular and generally range in size from 1 to 3cm but can reach up to 10cm across. The matrix, where present, is rock flour. Both clasts and matrix have undergone pervasive intense texturally-destructive silicification. Silicified clast boundaries are often difficult to distinguish from silicified matrix. Relic primary rock textures are only occasionally preserved. Cross sections based on diamond drill core data show that the breccia body is a shallow, upward flaring elongate body occurring along the main fault zone. Surface occurrences of this breccia coincide with the surface projection of the faults, which are themselves characterised by cataclasite zones ca. 5m wide with selvages of silicification and vuggy silica development (Fig. 3-30).

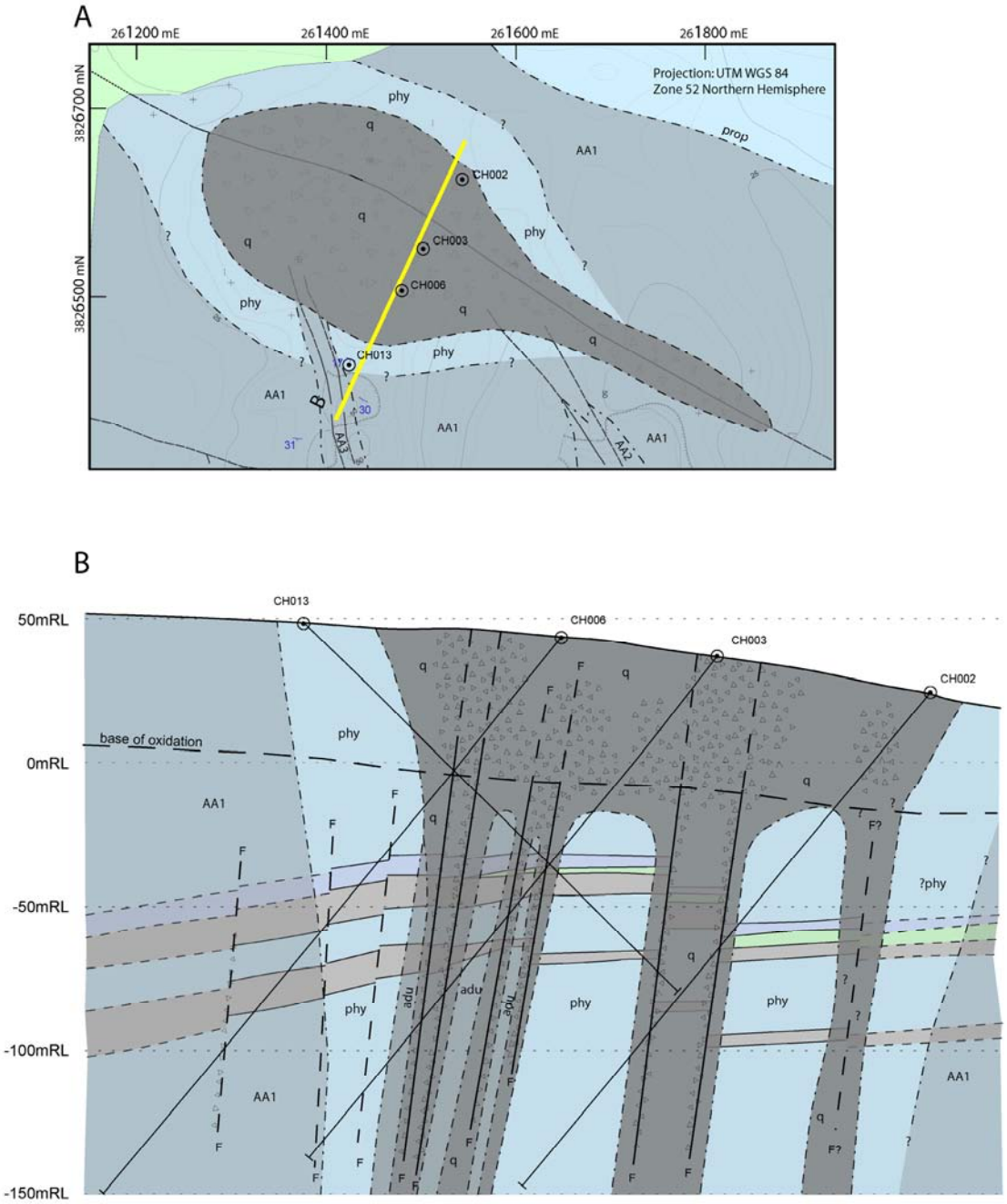

Fig. 3-30 Chunsan alteration zonation superimposed over geology and structure (from Fig. 2-35). Siliceous alteration, adjacent adularia alteration and related auriferous veining are localised around the faults that make up the Chunsan Fault Zone. The phyllic-adularia alteration and associated mineralisation at Chunsan overprints earlier advanced argillic alteration (see Section 3.4.2.2). Lithological unit labels have been removed (see Fig. 2-35 for labels). '**A**' and '**B**' views as per Figure 2-35. Alteration assemblages comprise the following: prop = propylitic; phy = phyllic; adv arg, AA1, AA2, AA3 = advanced argillic 1, 2, 3 (see Table 3-1); and q = siliceous. See main text for further detail.

Core siliceous, adularia and peripheral phyllic altered zones are focussed around the main faults that make up the Chunsan Fault Zone (Fig. 3-30), implying that the faults were the primary fluid ascent paths during this paragenetic stage. Relic patches of strongly advanced argillic altered rock, such as vuggy silica, are also focussed around these fault zones, implying that these faults were also important controls on the location of earlier advanced argillic alteration at Chunsan.

The location of high-grade quartz-adularia-sulfide-Au-Ag mineralised zones at Chunsan (e.g. Fig. 3-18) are more strongly developed within muddy horizons and/or within units that have been leached by earlier advanced argillic alteration, but which are located within core zones of siliceous-adularia alteration, coincident with the main fault zone at Chunsan.

The alteration zonation at Chunsan indicates that the main faults appear to be the primary control on fluid ascent, however, locally, the composition of the host rocks have had a significant control on the location of mineralisation. This will be explored further within Chapter 6.

Age data (this study; Chapter 4) shows that adularia growth and associated Au-Ag mineralisation at Eunsan, Moisan and Chunsan was essentially synchronous. Therefore, correlation with the structural setting of mineralisation at Eunsan (Section 3.5.3) suggests that mineralisation at Chunsan developed during district-scale stress regime 2, which is characterised by extension during transtension (Section 2.3; Table 3-3).

3.6 CLASSIFICATION OF THE SEONGSAN EPITHERMAL SYSTEMS

One of the ***main research aims*** of this thesis is to classify the epithermal systems of the Seongsan district, according to the geological characteristics highlighted by Cooke & Deyell (2003) and Hedenquist et al. (2000), and evaluate each as a classification method for epithermal systems.

It appears that current literature is shifting back towards descriptive nomenclature for classifying epithermal systems (Cooke & Deyell, 2003; Simmons et al., 2005), with less of a focus on the sulfidation state of the ore-forming fluids (Hedenquist et al., 2000). It is much easier to recognise alteration assemblages or infill textures and infer conditions of formation than undertake a detailed analysis of ore sulfide sulfidation state, assuming ore sulfides are even present.

In the Seongsan district, the Seongsan and Ogmaesan systems have little to no sulfide and therefore cannot be classified using the framework of Hedenquist et al. (2000). This highlights the limitations of a sulfidation-state classification system. Many more richly Au-Ag±Cu mineralised 'high-sulfidation' systems show multiple sulfidation states, where the ore-forming stage is associated with intermediate- to low-sulfidation fluids. Hence, sulfidation-state classification typically does not reflect fluid complexities, localised variations in sulfidation state or overprinting characteristics within a given system. Descriptive nomenclature, whether based on the framework of Cooke & Deyell (2003) or the more classical framework of Berger & Henley (1989), Hayba et al. (1985) and Heald et al. (1987), addresses these limitations and enables metalliferous and non-metalliferous mineralised and barren epithermal systems to be described and compared.

Table 3-4 shows descriptive nomenclature for the epithermal systems of the Seongsan district, based on the framework of Cooke & Deyell (2003), and where possible, the sulfidation-state of the ore forming fluids determined from sulfide assemblages; based on the framework of Hedenquist et al. (2000). Alternative classification from classical classification schemes are also shown for comparison.

	descriptive nomenclature	sulfidation-state (deposit type and mineralised sulfide state)	aka
Seongsan	sub-economic Au-Ag, massive, fault-hosted epithermal kaolinite-dickite-alunite deposit	high-sulfidation style deposit with high- to intermediate-sulfidation state sulfides, overprinted by minor occurrences of low-sulfidation style veining and alteration	acid-sulfate or alunite-kaolinite
Ogmaesan	barren Au-Ag, massive, breccia-hosted and stratabound epithermal kaolinite-dickite-alunite deposit	high-sulfidation style deposit (no Au-Ag-bearing sulfides)	acid-sulfate or alunite-kaolinite
Eunsan	adularia-illite altered, fault-hosted epithermal Au-Ag vein deposit	low-sulfidation style deposit with low- to intermediate-sulfidation state sulfides	adularia-sericite
Moisan	adularia-illite altered, fault- and cryptodome-hosted epithermal Au-Ag-(Te) ±Cu, ±Pb, ±Zn vein prospect	low-sulfidation style prospect with low- to intermediate-sulfidation state sulfides	adularia-sericite
Chunsan	kaolinite-quartz altered ± vuggy silica overprinted by adularia-illite altered, fault- and strata-bound epithermal Au-Ag prospect	high-sulfidation style alteration overprinted by low-sulfidation style prospect with low- to intermediate-sulfidation state sulfides	adularia-sericite

Table 3-4 Classification of the Seongsan district epithermal systems. Descriptive nomenclature is based on the framework of Cooke & Deyell (2003), adapted from earlier geological frameworks of Berger & Henley (1989), Hayba et al. (1985) and Heald et al. (1987). This descriptive nomenclature allows the varied nature of the different systems to be highlighted, which may not be the case with using traditional classification schemes. Sulfidation-state is from Hedenquist et al. (2000) incorporating both the common usage of the term to characterise a particular deposit as well as examination of the sulfidation-state of the metalliferous ore-forming sulfides. This highlights the potentially ambiguous and at times limiting nature of the sulfidation-state terms. Analogous references are also provided for reader familiarity.

3.7 SUMMARY OF RESULTS FROM THIS CHAPTER

This Chapter has documented the mineral assemblages, paragenetic relationships and geological setting of the gold-silver and clay-sulfate epithermal deposits and prospects in the Seongsan district. It has built on the results determined from Chapter 2, namely the lithostratigraphic and structural framework of the district. Key points from this Chapter include the recognition and documentation of two distinct hydrothermal events, one similar to acid-sulfate / high-sulfidation systems and the other similar to adularia-sericite / low-sulfidation epithermal systems (Table 3-3). Field relationships show that the adularia-sericite systems overprint the acid-sulfate systems, based on evidence from Seongsan and Chunsan. However, the exact age difference between them is unclear. Age dating (this study, Chapter 4) will resolve the absolute timing of these systems.

Analysis of the alteration, mineralisation and paragenesis of each system allows them to be classified according to the geological frameworks proposed by Cooke & Deyell (2003) and Hedenquist et al. (2000), and compared with earlier frameworks proposed by Berger & Henley (1989), Hayba et al. (1985) and Heald et al. (1987).

Integration of the paragenetic and geological settings for these systems (this Chapter), with earlier structural analyses of the district (Chapter 2) shows that the acid-sulfate systems are controlled by sinistral strike-slip faults and breccias that developed from wrenching during transpression (district-scale stress regime 1), while the phyllic-adularia systems are controlled by normal dip-slip faults that developed from extension during transtension (district-scale stress regime 2).

This determined framework for the epithermal systems of the Seongsan district (Chapters 2 and 3) allows subsequent geochronological and geochemical studies to be geologically well-constrained, which will aid in determining, among other things, whether or not these distinctly different epithermal systems are related parts of a single metallogenic event, or one or more different events.